Recurrent Holocene Paleoseismicity and Associated Land/Sea-Level Changes in South Central Alaska

External Grant Award # 06HQGR0033

Investigators: Ian Shennan, Antony Long and Natasha Barlow

Sea Level Research Unit
Department of Geography
University of Durham
Durham
DH1 3LE
United Kingdom

In collaboration with Rod Combellick

Alaska Division of Geological and Geophysical Surveys
Fairbanks, Alaska, USA

Telephone: +44 191 334 1934
Fax: +44 191 334 1801
Email: ian.shennan@durham.ac.uk
URL: http://www.geography.dur.ac.uk

Start date: 1st May 2006
End date: 30th April 2007

Key words: Paleoseismology, Recurrence interval, Surface Deformation

Research supported by the U.S. Geological Survey (USGS), Department of the Interior, under USGS award number 06HQGR0033. The views and conclusions contained in this document are those of the authors and should not be interpreted as necessarily representing the official policies, either expressed or implied, of the U.S. Government.

Recurrent Holocene Paleoseismicity and Associated Land/Sea-Level Changes in South Central Alaska

Ian Shennan, Antony Long and Natasha Barlow
Sea Level Research Unit, Department of Geography, University of Durham, Durham, DH1 3LE, UK
Telephone: +44 191 334 1934
Fax: +44 191 334 1801
Email: ian.shennan@durham.ac.uk
URL: http://www.geography.dur.ac.uk

Technical Abstract

In formulating this project on assessing regional earthquake hazards, we identified two research questions:

- Is there evidence for late Holocene great earthquakes with recurrence intervals ~100 years?
- Is the direction of pre-seismic land/sea-level movement the same as that observed during the co-seismic element of the deformation cycle?

Upon completion, we have answered the first one fully, the second with major qualifications and both raise new findings and new questions.

Analysis of ten peat-silt couplets at Girdwood shows that three do not indicate marsh submergence as the result of subsidence during a great earthquake. Without diatom analyses of these three peat-silt couplets the data would have suggested, incorrectly, six great earthquakes between ~3800 and ~2500 BP. This illustrates the danger of calculating recurrence intervals based only on lithology and radiocarbon ages. The remaining couplets result from co-seismic subsidence during seven great earthquakes in the last ~3800 years. With a low total number of radiocarbon analyses and individual probability distributions showing 200 – 300 year ranges we have insufficient data to determine recurrence intervals with rigorous statistical significance. The shortest interval between earthquakes is ~400 years (mean estimate, with ~180 years the minimum possible from present data). The longest interval is 800 to 1000 years, between the penultimate and AD 1964 earthquakes. Thus, we have one hypothesis of variable recurrence intervals from ~180 to 1000 years. Alternatively, for all of the earthquakes except AD 1964 a regular 600 year interval also fits the data. This hypothesis raises some intriguing questions: whether the great earthquake of 1964 followed an atypically long period of interseismic strain accumulation and that its pattern of rupture may not be typical of previous great earthquakes.

Severe storms and flooding limited our field investigations at Copper River Delta. While multiple silt-peat couplets show net subsidence through the mid- to late Holocene, a sharp boundary at the base of each peat layer indicates a hiatus and probable co-seismic uplift. Diatom and radiocarbon analyses show some support for co-seismic uplift and probable correlation with other sites, at Cape Suckling and upper Cook Inlet. Difficulties arise from poor diatom preservation, possible time lags in the onset of organic sediment accumulation following uplift, possible sediment erosion, highly variable freshwater and sediment discharge, salinity and channel migration in Copper River Delta. We will require modern diatom samples from Copper River Delta to assess the application of diatom transfer function models to reconstruct elevation change. Salinity variations and sediment discharge in the delta suggest a different relationship between diatom assemblages, sediment lithology and elevation compared to upper Cook Inlet. At this stage, we cannot accurately reconstruct the magnitude of relative land and sea-level changes through the different stages of each earthquake deformation cycle. This will require further research from areas experiencing co-seismic uplift.

Recurrent Holocene Paleoseismicity and Associated Land/Sea-Level Changes in South Central Alaska

Ian Shennan, Antony Long and Natasha Barlow
Sea Level Research Unit, Department of Geography, University of Durham, Durham, DH1 3LE, UK
Telephone: +44 191 334 1934
Fax: +44 191 334 1801
Email: ian.shennan@durham.ac.uk
URL: http://www.geography.dur.ac.uk

Non-Technical Abstract

Analysis of sediment cores at Girdwood reveals land subsidence during seven great earthquakes in the last 3800 years. They occur at variable intervals, possibly as short as 180 years or as long as 1000 years. The greatest interval is between the great 1964 earthquake and the preceding one. The 1964 earthquake may not be a typical event. We cannot yet identify large-scale patterns of surface deformation for pre-1964 earthquakes beyond upper Cook Inlet. Suitable sediments exist around Copper River Delta. Initial analysis allows some correlation but significant differences arise that require further investigation.

Contents

1. Context

Future earthquake prediction in the U.S. and minimisation of loss requires geologic evidence to estimate how often, where and what magnitude plate boundary earthquakes have occurred over the Holocene. This project applies temporal and vertical techniques to better understand long term records of Holocene paleoseismicity and associated land/sea-level movements in the greater Anchorage area and south-central Alaska from sedimentary sequences at Girdwood and the Copper River Delta (Figure 1). It builds on previous work undertaken by the principal investigators and focuses on two main research questions on regional earthquake hazards arising from the outcomes of our recent NEHRP projects:

- Is there evidence for late Holocene great earthquakes with recurrence intervals ~100 years?
- Is the direction of pre-seismic land/sea-level movement the same as that observed during the co-seismic element of the deformation cycle?

1.1 The earthquake deformation cycle in south-central Alaska

Coastal wetlands in the Pacific Northwest are excellent environments for registering Holocene seismic activity and associated relative sea-level changes due to their low energy depositional setting and their altitudinal control by sea level. The research status in south-central Alaska, on the Alaska-Aleutian plate boundary, differs in several ways to that found in the more intensively studied Cascadia subduction zone. Firstly, a large (M_w=9.2) and well-documented plate boundary earthquake struck this region on March 28th, 1964. Observations made before and after this event provide important information on pre- and post-seismic land and sea-level movements. Such observational data are lacking from the Juan de Fuca-North American plate boundary, where the last great boundary earthquake occurred some 300 years ago (Atwater and Hemphill-Haley, 1997). The 1964 Alaska earthquake therefore provides a well-defined benchmark against which earlier events can be compared and so improve our confidence in estimates of other Holocene earthquakes.

Using the framework of the 1964 event and the established criteria (Nelson *et al*., 1996) previous research (Hamilton and Shennan, 2005a; Shennan and Hamilton, 2006a) suggests a four phase earthquake deformation cycle (EDC) (as demonstrated in Figure 2) associated with a series of Holocene earthquakes in south-central Alaska. The research presents a chronology of palaeo-earthquakes from four sites, Girdwood, Anchorage, Kenai and Kasilof (Hamilton and Shennan, 2005a; Hamilton *et al*., 2005; Hamilton and Shennan, 2005b; Shennan and Hamilton, 2006a).

1.2 Late Holocene earthquake recurrence intervals

Our previous investigations of multiple sections at Girdwood (Figure 3) provide the most complete record of Holocene great earthquakes. It lies close to the area of maximum subsidence in AD1964 and earthquakes ~900, ~1500, ~2100, ~2500 and ~3300 BP record subsidence of the same order (Shennan and Hamilton, 2006a). Two further peat-silt couplets with similar lithostratigraphy, peat C ~2600 BP and peat B ~2800 BP suggest possible co-seismic subsidence but diatoms from the overlying silt in each case indicate freshwater assemblages and not co-seismic land subsidence to a level within the intertidal zone.

However, evidence for variable subsidence with the ~2100 BP great earthquake (Hamilton and Shennan, 2005a; Shennan and Hamilton, 2006a), derived from diatom analyses at three separate locations at Girdwood (Peat E Table 1), suggest that peat B and peat C required further study.

Locations GW-1, GW-2 and GW-3 lie on the north shore of Turnagain Arm, at the junction with the valley of Glacier Creek (Figure 3). For the ~2100 BP great earthquake, represented by peat E,

location GW-1, closest to the central axis of Glacier Creek valley, records the greatest co-seismic subsidence, ~1.2 m. Subsidence diminishes to ~0.8 m at the intermediate location, GW-2. GW-3, closest to the north side of the valley, records a similar lithology, peat with a sharp upper contact overlain by grey silt (Figure 3), but the silt contains a freshwater diatom assemblage for which we have no modern analogue. If the sample from GW-3 were the only one studied for this peat-silt couplet we could not have demonstrated co-seismic subsidence.

Table 1 – Summary of ages and co-seismic land elevation changes at Girdwood associated with great earthquakes ~3300 – 2100 BP

Peat	Age	GW-3	GW-2	GW-1
E	~2100 BP	No tidal submergence	-0.79±0.29 m	-1.20±0.34 m
D	~2500 BP	Not sampled	-1.48±0.42 m	-1.42±0.34 m
C	~2600 BP	Not sampled	No tidal submergence	Peat not present
B	~2800 BP	Not sampled	No tidal submergence	No tidal submergence
A	~3300 BP	Not sampled	-1.60±0.32 m	-1.36±0.3 m

In order to test the hypothesis that great earthquakes can occur ~100 yr apart (research question one) within this project we trace the extent of peat layers GW-B and GW-C across the south side of Glacier Creek. If both record overlying silt with inter-tidal diatom assemblages rather than freshwater assemblages, a spatial trend observed for the ~2100 BP peat, GW-E, could indicate three great earthquakes between ~2800 and ~2500 BP.

1.3 A four-phase earthquake deformation cycle of land/sea-level movement

One of our most critical findings to date is that all of the peat-silt couplets that record great earthquakes in the last 3300 years have a precursor: evidence of pre-seismic land subsidence in contrast to relative sea-level fall through the preceding interseismic period of each earthquake cycle. Diatom changes prior to the 1964 earthquake at Girdwood 33 (Zong *et al*., 2003) show relative sea-level rise commencing ~AD 1952. Direct observations of relative sea-level changes before 1964 also offer support for pre-seismic subsidence. Karlstrom (1964) recorded storm tides first flooded the marsh surface at Girdwood in AD 1953, depositing thin surface layers of silt that became progressively thicker each year thereafter. Loss on ignition results for Girdwood 33, section sampled in AD 1998 reflects this in the top 5cm of the peat layer (Zong *et al*., 2003). Applying the same microfossil approaches to all the peat-silt couplets we have studied shows that pre-seismic relative sea-level rise a common feature around Upper Cook Inlet (Shennan and Hamilton, 2006a).

We previously considered and tested alternative explanations for the apparent pre-seismic land subsidence; including the possibility of sediment mixing and temporary sea level changes associated with the El Nino Southern Oscillation (ENSO) (Hamilton *et al*., 2005). However, we concluded that pre-seismic change, relative sea-level rise/land subsidence, is a common feature at sites experiencing co-seismic subsidence during great earthquakes in the late Holocene. We are less confident in understanding the mechanism. A possible mechanism involves episodic aseismic slip on the seismogenic plate boundary. Observations and models of aseismic slip come from Cascadia (Dragert *et al*., 2001; Miller *et al*., 2002) and Japan (Hori *et al*., 2004; Kato, 2003; Uchida *et al*., 2004), though timescales range from a few days to a few years rather than a decade; e.g. tide gauge data record several centimetres of aseismic subsidence during a five year period before the 1994 Hokkaido-Toho-Oki earthquake (M_w=8.3) (Katsumata *et al*., 2002).

In order to gain further insight into possible mechanisms we test a hypothesis in which both pre-seismic and co-seismic movements result from slip on the plate boundary and the direction of pre-seismic land/sea-level movement is the same, but of different magnitude, as the co-seismic movement (research question two). To do this we evaluate the four-stage earthquake deformation cycle model at a site in the zone of co-seismic land uplift, where pre-seismic change should be relative land uplift. The AD1964 earthquake produced ~2 m coseismic uplift at Copper River Delta (Plafker, 1969; Plafker *et al*., 1992b). Applying the earthquake deformation model, co-seismic uplift raises the tidal flat to above high tide level so peat starts to form, followed by gradual land subsidence and peat submergence to the interseismic phase. By re-sampling and dating the series of silt-peat units recorded by Plafker *et al*., (1992) we test this hypothesis and similarities between the AD1964, ~900BP and ~1500BP great earthquakes recorded at the sites around Cook Inlet (Shennan and Hamilton, 2006a).

2. Field Investigations

Field investigation took place during May (Girdwood) and August/September (Girdwood and Copper River Delta) 2006 to collect both modern and Holocene sediments.

2.1 Girdwood (Research Question 1)

A series of cores, using a 20mm gouge, at Girdwood marsh to the south of Glacier Creek (Figure 4) trace the horizontal extent of the Holocene peat layers seen in previous cores to the north. Cores extend 685 cm to 846 cm from the surface (with the exception of GW/06/2 and GW/06/3 where gravel or cobbles at ~500 cm ended coring) and demonstrate multiple peat-silt couplets with sharp upper contacts to each peat unit. Selected sections of cores GW/06/1, GW/06/4, GW/06/5 and GW/06/6 were sealed in plastic for transport to Durham and subsequent analysis. Previous work (Hamilton and Shennan, 2005a) already provides a comprehensive database of modern samples for Upper Cook Inlet.

2.2 Copper River Delta (Research Question 2)

We aimed to resample the Alaganik Slough stratigraphy, by tidal creek exposures and coring, to trace the lateral extent of the units and collect a minimum of two peat layers documented by Plafker *et al*. (1992). The day before our arrival in Cordova severe storms and resulting floods washed away a section of the Copper River Highway to our field site. We chartered a small aircraft to determine that the site was still intact if we could get across the breached road section. Consequently, our fieldwork was limited to the final two days once the road section was repaired. Heavy rain continued and the Alaganik Slough was running well above normal.

At low tide on the first day we were able to trace the top peat layer for ~2km along the Slough. Lower peat layers as reported by Plafker *et al*. (1992b) were not visible. Further heavy rain, continuous from the afternoon of the first day through the whole of the second meant than Alaganik Slough was near bank full stage, over 3.5 m above normal low tide conditions. With the possibility that the road would be washed away again while we were at Alaganik Slough, access to the site and time were very restricted. All sections were submerged but using a combination of a 50mm piston and 20mm gouge corers we sampled one core of Holocene sediments to 335 cm below ground surface (Figure 5).

In order to assess the performance of our transfer function models, developed for Cook Inlet, applied to Copper River Delta sediments, we require modern diatom samples from the area. The tidal flat and marsh at Hartney Bay (~32km from Alaganik Slough) provided the most suitable location (Figure 6), avoiding the freshwater flood discharge around Copper River Delta itself. While the Copper River

Highway was being repaired we collected twenty-two modern sediment samples, each levelled to high tide and converted to elevations relative to Mean Higher High Water (MHHW) using NOAA data (http://co-ops.nos.noaa.gov) for the tide gauge at Cordova, ~5 km away. MHHW allows comparison with the modern samples from Cook Inlet (Hamilton and Shennan, 2005a).

3. Methods

We follow standard procedures, previously reported (Shennan *et al*., 2004) and reproduced as Appendix A. Laboratory analysis for both research questions focuses on diatom analysis of the modern and fossil sediments and radiocarbon dating.

4. Results

4.1 Research Question 1 - Is there evidence for late Holocene great earthquakes with recurrence intervals ~100 years?

Seven cores record the lateral variability of peat layers in the central section of Girdwood marsh, between Glacier Creek and Virgin Creek (Figures 4 and 7). Allowing for the vertical exaggeration of the figure, there is a degree of consistency across over at least 2km, from GW-2 to GW/06/6. Nevertheless, it is impossible to correlate peat layers on lithology alone, by counting down from the surface. We correlate peat layers using radiocarbon ages (Table 2) and diatom assemblages. Without these chrono- and bio-stratigraphic data, the lowermost peat layers in the central marsh may appear equivalent to peat A and B in the northern section, whereas they are older, shown by their radiocarbon ages (Table 1). In the northern section, peat D and peat A are both overlain by silt with intertidal diatoms. In the central section, GW/06/1, 4, 5 and 6, they are likewise overlain by silt with intertidal diatoms (Figures 8 and 9) and radiocarbon ages confirm their respective correlation. Peat Y and peat Z represent new evidence of possible co-seismic submergence to extend the record of Holocene palaeoseismicity at Girdwood.

Table 2 – Radiocarbon results for Girdwood for cores taken 2006

Site	Lab code (Beta-)	Stratigraphic context	Laboratory reported ^{14}C age ±1σ	Calibrated age BP Median age followed by minimum and maximum ages of 95% range		
GW/06/6	223768	Top of peat 'D'	2490 ±40	2576	2729	2365
GW/06/1	223763	Top of peat 'A'	3010 ±40	3216	3335	3078
GW/06/5	223766	Top of peat 'A'	3020 ±40	3232	3344	3079
GW/06/6	223767	Top of peat 'A'	2930 ±40	3090	3213	2959
GW/06/5	223765	Top of peat 'Z'	3220 ±40	3437	3556	3366
GW/06/5	223764	Top of peat 'Y'	3490 ±40	3765	3867	3643

Peat layers A and D provide the critical correlation from the northern marsh to the central marsh. The peat between A and D in cores GW/06/4 and 5 is overlain by silt with freshwater diatoms (Figure 10). Indeed, at no location do we find a peat overlain by silt with intertidal diatoms stratigraphically between peat A and peat D. Therefore we have no evidence to support the hypothesis for a coseismic origin for the submergence of either peat B or C and therefore, on the evidence of freshwater diatoms from cores GW/06/04 (Figure 10), GW-1 and GW-2 (Hamilton and Shennan, 2005a) we reject the hypothesis of three great earthquakes between ~2800 and ~2500 BP.

The peat-silt couplet a few centimetres below peat A in cores GW/06/1, 4, 5 and 6 (Figure 7), peat Z, only has freshwater diatom assemblages (Figure 11) within both the peat and overlying silt, so, as with peat B and peat C, does not indicate co-seismic subsidence.

In contrast, peat Y, records marsh subsidence. It is not a fully developed peat, rather a highly organic silt with fine herbaceous rootlets. In each of the four cores (Figure 7) it has a sharp upper boundary. Based on this lithology we would suggest it represents low salt marsh prior to co-seismic subsidence. Diatom analyses from two cores show very similar assemblages, in terms of the main species present and their overall trends (Figures 12 and 13).

Reconstructions of relative sea-level change from the transfer function suggest co-seismic subsidence ~1.0±0.3 m for both peat D and peat A (Figure 14), less subsidence than recorded in 1964, ~1.5 m regional subsidence and up to an extra 0.9 m due to localised sediment consolidation (Plafker, 1969; Plafker *et al*., 1969). Smaller changes in individual species frequencies occur across the top of peat Y compared to those across the top of peat A and transfer function reconstructions indicate ~0.7±0.3 m co-seismic subsidence (Figure 14).

These new lithostratigraphic, biostratigraphic and radiocarbon data extend the record of Holocene paleoseismicity for the area and address previous uncertainties about possible short, ~100 year, recurrence intervals between great earthquakes.

4.1.1 Great earthquake recurrence intervals

Analysis of ten peat-silt couplets correlated across various parts of Girdwood marsh (Figure 7) shows that three, Z, B and C, do not fulfil the criteria of Nelson *et al* (1996) as indicating marsh submergence the result of co-seismic subsidence. Without diatom analyses of these three peat-silt couplets the data would have suggested, incorrectly, six great earthquakes, represented by peat Y through peat D, between ~3800 and ~2500 BP. This illustrates the danger of calculating recurrence intervals based only on lithology and radiocarbon ages.

We conclude that the remaining couplets result from co-seismic subsidence during seven great earthquakes in the last ~3800 years (Figure 15). Estimates of subsidence at Girdwood range between ~0.7±0.3 m and ~1.6±0.3 m (Figure 14 and Table 1 of Shennan and Hamilton, 2006). With a low total number of radiocarbon analyses and individual probability distributions showing 200 – 300 year ranges (Figure 15) we have insufficient data to determine recurrence intervals with rigorous statistical significance. The shortest interval between occurs between D and E, ~400 years, with ~180 years the minimum possible from present data. The longest interval is 800 to 1000 years, between peat G and peat H, representing the penultimate and AD 1964 earthquakes. Thus, we have one hypothesis of variable recurrence intervals from ~180 to 1000 years. Alternatively, for all of the earthquakes except AD 1964 a regular 600 year interval also fits the data (Figure 15). This hypothesis raises some intriguing questions: whether the great earthquake of 1964 followed an atypically long period of interseismic strain accumulation and that its pattern of rupture may not be typical of previous great earthquakes.

4.2 Research Question 2 - Is the direction of pre-seismic land/sea-level movement the same as that observed during the co-seismic element of the deformation cycle?

The core from Alaganik Slough records two peat layers each with a sharp lower contact overlying silt (Figure 16). The sharp contact indicates an hiatus of unknown duration. Radiocarbon dates at the base of each peat layer indicate peat growth commencing ~600 and ~1500 yrs BP (Table 3). The older age, peat A, correlates with Plafker *et al*'s (1992b) bulk date of 1270-1630 yrs BP from Copper

River Delta and with others for a coseismic subsidence ~1500 BP in upper Cook Inlet (Shennan and Hamilton, 2006a). One sample from peat B partially overlaps with that dated 895-665 BP by Plafker *et al*. (1992b). In upper Cook Inlet the penultimate great earthquake occurred ~900 BP (Shennan and Hamilton, 2006a). An additional date from the base of peat B gives an anomalous value of 425-0 BP (Table 3), which suggests possible contamination, for example penetration from the roots of younger vegetation. We cannot therefore be confident in directly correlating this layer with the paleoseismicity record from Cook Inlet. Our 569-682 BP sample may indicate a delay in organic sediment accumulation on the raised clastic sediment. In contrast, at Cape Suckling, a tidal marsh sequence records coseismic uplift followed by organic accumulation dated 930-740 BP (Shennan and Hamilton, 2006b; Shennan and Hamilton, 2006c).

Table 3 – Radiocarbon results for Alaganik Slough core taken 2006

Site	Lab code (Beta-)	Stratigraphic context	Laboratory reported ^{14}C age ±1σ	Calibrated age BP Median age followed by minimum and maximum ages of 95% range		
AS/06/1	223759	Base of peat 'B'	220 ±40	192	0	425
AS/06/1	223760	Base of peat 'B'	700 ±40	661	569	682
AS/06/1	228853	Near base of peat 'A'	1350 ±60	1273	1182	1315
AS/06/1	223761	Base of peat 'A'	1610 ±40	1488	1417	1541

Diatom assemblages in peat B (Figure 17) shows a shift in salinity preferences across the silt-peat boundary. The overlying peat is slightly more dominated by oligohalobian-indifferent and halophobe species than the underlying silt, indicating relative land uplift. When we use the modern diatom dataset from upper Cook Inlet (Hamilton and Shennan, 2005a) to reconstruct land/sea-level change (Figure 18i) we see little elevation change through the core, without the degree of uplift suggested by the lithology or if we were to expect a similar pattern of co-seismic deformation compared to AD 1964 (Figure 1).

This raises the critical question of whether we can use the locally-developed diatom transfer function models from Cook Inlet to improve the vertical (elevation) accuracy and precision of geologic estimates of land level changes from great Holocene plate boundary earthquakes elsewhere in Alaska. In our Cook Inlet investigation we use the minimum dissimilarity coefficient, from the Modern Analogue Technique (Birks, 1995), as an indication of goodness-of-fit between each fossil sample and our modern dataset. Applying this approach to the Alaganik Slough shows no fossil samples having a close modern analogue.

To try to improve the model we apply a second transfer function, combining modern data from upper Cook Inlet with twenty-two samples collected for this project from Hartney Bay (Figures 19 and 20). Reconstructed elevations have a slightly larger error term for the fossil silt samples (Figure 18ii) and again no close modern analogue for any of the fossil assemblages. As Hartney Bay only contains one sample from an elevation above SWLI 225 (Figure 21), the combined dataset has little impact on the reconstruction of samples from the peat. The pattern of elevation change reported by the two models differs slightly, though both demonstrate limited elevation change across the silt-peat boundary.

These results raise significant questions regarding the vertical (elevation) accuracy and precision of geologic estimates of land level changes in Copper River Delta from great Holocene plate boundary earthquakes and their correlation with evidence from other locations. First we have the issue of the duration of any hiatus following land uplift. If we assume silt-peat couplet B represents coseismic uplift ~900 BP the radiocarbon samples suggest an hiatus equivalent to ~200 yr or more. This could arise from numerous processes, ranging from no sedimentation to sediment erosion. Given the dynamics of Copper River Delta we can only speculate. Within this ~200 yr period models of multiple earthquake deformation cycles suggest rapid post-seismic and interseismic subsidence, so the small

shift in elevation (Figure 18) may be a good estimate. Given mid-Holocene sediment sequences of multiple peat-silt couplets we know there is net subsidence in Copper River Delta within each earthquake cycle (Plafker *et al*., 1992a).

Alternatively, our present transfer function model may not be applicable to Copper River Delta. For example, all fossil samples have no close modern analogue and the samples from Hartney Bay increase the scatter of data points in the observed against prediction elevation plots (Figure 21). If we consider the dominant species in silt-peat couplet B we see *Diploneis ovalis* within the fossil silt at Alaganik Slough, whereas in the modern environment of upper Cook Inlet *Diploneis ovalis* is present at elevations (SWLI >235) normally associated with peat accumulation. This suggests different controls beyond elevation on the relationships between sediment lithology and diatom zonation in Copper River Delta, Hartney Bay and upper Cook Inlet. Figure 22 shows the difference in salinity ranges reported for upper Cook Inlet, Hartney Bay and Copper River Delta. Seasonal glacial melt water in Copper River Delta results in summer salinity values in Peter Dahl Slough as low as 2 psu (Powers *et al*., 2002), far fresher than the waters surrounding the contemporary sample sites of upper Cook Inlet and Hartney Bay. In addition, Copper River Delta is a highly turbid environment, recording between 50 and 400 nephelometer turbidity units (NTU) compared to Hartney Bay where it is typically <20 NTU (Powers *et al*., 2006). We therefore propose that the sampled contemporary environments differ too greatly from the fossil ones to present a suitable modern analogue. Consequently, we suggest that it is not possible to accurately reconstruct land/sea-level changes in Copper River Delta at present without a modern diatom dataset from Alaganik Slough.

The lower silt-peat biostratigraphy shows very limited preservation of diatoms. At no location in the core are we able to count an assemblage with over 250 valves (Figure 23). Though we have recorded the counted diatoms, there are not enough to make it statistically viable to reconstruct land/sea-level changes for silt-peat couplet A.

5. Conclusions

In formulating this project on assessing regional earthquake hazards, we identified two research questions:

- Is there evidence for late Holocene great earthquakes with recurrence intervals ~100 years?
- Is the direction of pre-seismic land/sea-level movement the same as that observed during the co-seismic element of the deformation cycle?

In completing the project, we have answered the first one fully, the second with major qualifications and both raise new finding and new questions.

Analysis of ten peat-silt couplets at Girdwood shows that three do not indicate marsh submergence as the result of subsidence during a great earthquake. Without diatom analyses of these three peat-silt couplets the data would have suggested, incorrectly, six great earthquakes between ~3800 and ~2500 BP. This illustrates the danger of calculating recurrence intervals based only on lithology and radiocarbon ages. The remaining couplets result from co-seismic subsidence during seven great earthquakes in the last ~3800 years (Figure 15). With a low total number of radiocarbon analyses and individual probability distributions showing 200 – 300 year ranges we have insufficient data to determine recurrence intervals with rigorous statistical significance. The shortest interval occurs between D and E, ~400 years, with ~180 years the minimum possible from present data. The longest interval is 800 to 1000 years, between peat G and peat H, representing the penultimate and AD 1964 earthquakes. Thus, we have one hypothesis of variable recurrence intervals from ~180 to 1000 years. Alternatively, for all of the earthquakes except AD 1964 a regular 600 year interval also fits the data (Figure 15). This hypothesis raises some intriguing questions: whether the great earthquake of 1964

followed an atypically long period of interseismic strain accumulation and that its pattern of rupture may not be typical of previous great earthquakes.

Severe storms and flooding limited our field investigations at Copper River Delta. While multiple silt-peat couplets show net subsidence through the mid- to late Holocene, a sharp boundary at the base of each peat layer indicates a hiatus and probable co-seismic uplift. Diatom and radiocarbon analyses show some support for co-seismic uplift and probable correlation with other sites, at Cape Suckling and upper Cook Inlet. Difficulties arise from poor diatom preservation, possible time lags in the onset of organic sediment accumulation following uplift, possible sediment erosion, highly variable freshwater and sediment discharge, salinity and channel migration in Copper River Delta. We will require modern diatom samples from Copper River Delta to assess the application of diatom transfer function models to reconstruct elevation change. Salinity variations and sediment discharge in the delta suggest a different relationship between diatom assemblages, sediment lithology and elevation compared to upper Cook Inlet. At this stage, we cannot accurately reconstruct the magnitude of relative land and sea-level changes through the different stages of each earthquake deformation cycle. This will require:

1. modern diatom samples from Copper River Delta
2. analysis of the same silt-peat couplet at different locations in the delta to minimise possible effects of poor diatom preservation, time-lags in the onset of organic sediment accumulation following uplift, sediment erosion, highly variable freshwater and sediment discharge, salinity gradients and channel migration
3. comparison with other sites from the zone of co-seismic uplift but outside of Copper River Delta (where we expect the limitations in point 2 to be less severe), such at Cape Suckling or near Cordova.

6. Appendix A

See our previous report (Shennan *et al*., 2004) for bibliographic details of references cited only in this appendix.

6.1 Microfossil analysis

Analysis of the surface samples from Hartney Bay allows development of a modern data set, ranging from tidal flat through to raised bog environments to compare to our published data (Hamilton and Shennan, 2005a).

Sampling intervals of fossil cores varied from 0.5 to 2cm.

Preparation of diatom samples followed standard laboratory methods (Palmer & Abbott, 1986) with a minimum count of 250 diatom valves possible for most samples. Diatom identification used Van der Werff and Huls (1958-1974) together with supplementary texts of Denys (1991), Hartley *et al*. (1996), Hemphill-Haley (1993) and Patrick and Reimer (1966, 1975). TILIA (version 2.0 b5; Grimm, 1993) allows plotting of results and the halobian classification system divides the diatom species into five categories of salt tolerance (Table 4).

In broad terms, the order of salinity classes should reflect the change from tidal flat through salt marsh, to freshwater marsh and bog. The marine (polyhalobous class) and brackish (mesohalobous class) groups usually dominate tidal flat environments and freshwater groups tolerant of different degrees of saline inundation (oligohalobous-halophile and oligohalobous-indifferent classes) become dominant through the transition from salt marsh to freshwater marsh (e.g. Zong *et al*., 2003). Salt-intolerant species (halophobous class) characterise the most landward communities, including acidic bog above the level of the highest tides. No attempt was made to separate out the allochthonous and

autochthonous diatoms because we assume that processes acting today are the same as those acting in the past. According to Sawai (2001), the removal of dead diatoms by tidal currents may result in a residual assemblage for the surface tidal flat samples. However, this would also have occurred in the fossil tidal flat samples recorded by the silt units.

Table 4 – The halobian classification scheme (Hemphill-Haley, 1993)

Classification	Salinity range (‰)	Description
Polyhalobous	> 30	Marine
Mesohalobous	0.2 to 30	Brackish
Oligohalobous - halophile	< 0.2	Freshwater – stimulated at low salinity
Oligohalobous - indifferent	< 0.2	Freshwater – tolerates low salinity
Halophobous	0	Salt-intolerant

Microfossils help distinguish between seismic and non-seismic origins of peat-silt couplets (e.g. Long & Shennan, 1994; Nelson *et al*., 1996) and the tendency approach (e.g. Shennan, 1986) defines periods within the EDC model (e.g. Long & Shennan, 1994). A positive sea-level tendency represents an increase in marine influence and a negative sea-level tendency represents a decrease in marine influence.

6.2 Radiocarbon dating

In situ macrofossils were used for AMS radiocarbon dating. CALIB 5.0.1 (Stuiver & Reimer, 1993) calibrates the radiocarbon results to calendar years before present using the atmospheric decadal data set (file INTCAL04.14C, Reimer *et al*., 2004) and the 95% probability distribution method. In addition we recalibrated the ages reported in Hamilton and Shennan (2005a) using the INTCAL04.14C data set to allow comparison with the dates reported for this project. Calibrated ages are reported as the range between the calculated minimum and maximum value, with the median age marked on figures.

6.3 Numerical Techniques

6.3.1 Transfer function

Numerical techniques establish the relationship between contemporary diatom data and elevation (m) relative to MHHW and allow comparisons between the contemporary data set and every fossil sample analysed. These provide quantitative estimates of relative sea-level change throughout the entire profile, rather than just at stratigraphic boundaries.

Contemporary distribution of diatoms from tidal flat to freshwater environments allows development of a transfer function to reconstruct the magnitude of relative land and sea-level changes. Birks (1995) reviews the basic principles of quantitative environmental reconstruction. In this study, the primary aim of a transfer function (Imbrie & Kipp, 1971) is to predict environmental variables for a fossil sample using a modern training set. This involves regression that models the relationship between contemporary diatom assemblages and their associated environmental variables of interest. Calibration then uses this relationship to transform the fossil data into quantitative estimates of past environmental variables.

Most methods assume a linear or unimodal taxon-environment response model. In nature, most species-environment relationships are unimodal, as most taxa survive best in optimum environmental

conditions (Birks, 1995). However, if the data spans only a narrow range of environmental variation then it may appear linear (Birks, 1995). For reconstruction purposes, it is essential to estimate the gradient length for the environmental variables of interest. CONOCO (version 4.5; ter Braak & Smilauer, 2002) uses Detrended Canonical Correspondence Analysis (DCCA) to estimate the gradient length in standard deviation (SD) units by detrending segments with non-linear rescaling. Gradient length is important as it governs what transfer function models are suitable for the data set.

If the gradient length is short (2 SD units or less), linear regression and calibration methods are appropriate, for example, Partial Least Squares (PLS). If the gradient length is longer (2 SD units or more), several taxa have their optima located within the gradient and unimodal based methods of regression and calibration are best (Birks, 1995). Such models include Weighted Averaging (WA), Weighted Averaging with Tolerance Downweighting (WA-TOL) and Weighted Averaging-Partial Least Squares (WA-PLS), all available within the software package C2 (Juggins, 2003).

Statistical parameters produced during regression and calibration includes the coefficient of determination (r^2) that measures the strength of a relationship between observed and inferred values (Birks, 1995). The Root Mean Square Error of Prediction (RMSEP) measures the predictive abilities of the training set and is calculated by a method called bootstrapping (ter Braak & Juggins, 1993).

When calculating a relative sea-level change between two fossil samples, the change in elevation is simply the difference between the two reconstructed values and calculation of the associated error term uses the formula (Preuss, 1979):

$$\sqrt{(\text{error term } 1^2 + \text{error term } 2^2)}$$

6.3.2 Modern analogue technique

The modern analogue technique (MAT) quantifies the similarity between fossil assemblages and the modern training set (Birks *et al*., 1990) and is particularly useful in identifying whether fossil samples possess good modern analogues (e.g. Birks, 1995; Edwards & Horton, 2000; Zong *et al*., 2003). The computer program C2 (Juggins, 2003) models the full contemporary diatom data set against each fossil data set and determines the minimum dissimilarity coefficient for each fossil sample.

6. References

Atwater, B. F., and Hemphill-Haley, E. (1997). Recurrence intervals for great earthquakes of the past 3,500 years at northeastern Willapa Bay, Washington. *U.S. Geological Survey Professional Paper* **1576,** 1-108.

Birks, H. J. B. (1995). Quantitative palaeoenvironmental reconstructions. *In* "Statistical modelling of Quaternary Science data." (D. Maddy, and J. S. Brew, Eds.), pp. 161-254. Technical Guide 5. Quaternary Research Association., Cambridge.

Dragert, H., Wang, K., and James, T. S. (2001). A silent slip event on the deeper Cascadia subduction interface. *Science* **292,** 1525-1528.

Atwater, B. F., and Hemphill-Haley, E. (1997). Recurrence intervals for great earthquakes of the past 3,500 years at northeastern Willapa Bay, Washington. *U.S. Geological Survey Professional Paper* **1576,** 1-108.

Birks, H. J. B. (1995). Quantitative palaeoenvironmental reconstructions. *In* "Statistical modelling of Quaternary Science data." (D. Maddy, and J. S. Brew, Eds.), pp. 161-254. Technical Guide 5. Quaternary Research Association., Cambridge.

Dragert, H., Wang, K., and James, T. S. (2001). A silent slip event on the deeper Cascadia subduction interface. *Science* **292,** 1525-1528.

Hamilton, S., and Shennan, I. (2005a). Late Holocene relative sea-level changes and the earthquake deformation cycle around upper Cook Inlet, Alaska. *Quaternary Science Reviews* **24,** 1479-1498.

Hamilton, S., Shennan, I., Combellick, R., Mulholland, J., and Noble, C. (2005). Evidence for two great earthquakes at Anchorage, Alaska and implications for multiple great earthquakes through the Holocene. *Quaternary Science Reviews* **24,** 2050-2068.

Hamilton, S. L., and Shennan, I. (2005b). Late Holocene great earthquakes and relative sea-level change at Kenai, southern Alaska. *Journal of Quaternary Science* **20,** 95-111.

Hori, T., Kato, N., Hirahara, K., Baba, T., and Kaneda, Y. (2004). A numerical simulation of earthquake cycles along the Nankai Trough in southwest Japan: lateral variation in frictional property due to the slab geometry controls the nucleation position. *Earth and Planetary Science Letters* **228,** 215-226.

Karlstrom, T. N. V. (1964). Quaternary geology of the Kenai lowland and the glacial history of the Cook Inlet region, Alaska. *US Geological Survey Professional Paper* **443,** 1-69.

Kato, N. (2003). A possible model for large preseismic slip on a deeper extension of a seismic rupture plane. *Earth and Planetary Science Letters* **216,** 17-25.

Katsumata, K., Kasahara, M., Ozawa, S., and Ivashchenko, A. (2002). A five years super-slow aseismic precursor model for the 1994 M8.3 Hokkaido-Toho-Oki lithospheric earthquake based on tide gauge data. *Geophysical Research Letters* **29,** 32-1 to 32-4.

Miller, M. M., Melbourne, T., Johnson, D. J., and Sumner, W. Q. (2002). Periodic slow earthquakes from the Cascadia subduction zone. *Science* **295,** 2423.

Nelson, A. R., Shennan, I., and Long, A. J. (1996). Identifying coseismic subsidence in tidal-wetland stratigraphic sequences at the Cascadia subduction zone of western North America. *Journal of Geophysical Research* **101,** 6115-6135.

Plafker, G. (1969). Tectonics of the March 27, 1964, Alaska earthquake. *U.S. Geological Survey Professional Paper* **543-I,** 74.

Plafker, G., Kachadoorian, R., Eckel, E. B., and Mayo, L. R. (1969). Effects of the earthquake of march 27, 1964 on various communities. *US Geological Survey Professional Paper* **542-G,** 1-50.

Plafker, G., Lajoie, K. R., and Rubin, M. (1992a). Determining intervals of great subduction zone earthquakes in southern Alaska by radiocarbon dating. *In* "Radiocarbon after four decades. An interdisciplinary perspective." (R. E. Taylor, A. Long, and R. S. Kra, Eds.), pp. 436-452. Springer Verlag, New York.

Plafker, G., Lajoie, K. R., and Rubin, M. (1992b). Determining recurrence intervals of great subduction

zone earthquakes in Southern Alaska by radiocarbon dating. *In* "Radiocarbon after four decades: An interdisciplinary perspective." (R. E. Taylor, A. Long, and R. S. Kra, Eds.), pp. 436-453. Springer-Verlag, New York.

Powers, S. P., Bishop, M. A., Grabowski, J. H., and Peterson, C. H. (2002). Intertidal benthic resources of the Copper River Delta, Alaska, USA. *Journal of Sea Research* **47,** 13-23.

Powers, S. P., Bishop, M. A., Grabowski, J. H., and Peterson, C. H. (2006). Distribution of the invasive bivalve Mya arenaria L. on intertidal flats of southcentral Alaska. *Journal of Sea Research* **55,** 207-216.

Ramsey, C. B. (2001). Development of the radiocarbon calibration program. *Radiocarbon* **43,** 355-363.

Reimer, P. J., Baillie, M. G. L., Bard, E., Bayliss, A., Beck, J. W., Bertrand, C. J. H., Blackwell, P. G., Buck, C. E., Burr, G. S., Cutler, K. B., Damon, P. E., Edwards, R. L., Fairbanks, R. G., Friedrich, M., Guilderson, T. P., Hogg, A. G., Hughen, K. A., Kromer, B., McCormac, G., Manning, S., Ramsey, C. B., Reimer, R. W., Remmele, S., Southon, J. R., Stuiver, M., Talamo, S., Taylor, F. W., van der Plicht, J., and Weyhenmeyer, C. E. (2004). IntCal04 Terrestrial Radiocarbon Age Calibration, 0-26 Cal Kyr BP. *Radiocarbon* **46,** 1029-1058.

Shennan, I., and Hamilton, S. (2006a). Coseismic and pre-seismic subsidence associated with great earthquakes in Alaska. *Quaternary Science Reviews* **25,** 1-8.

Shennan, I., and Hamilton, S. L. (2006b). Holocene sea-level changes, earthquakes and tsunami around Bering Glacier. In: Bering Glacier to Glacier Bay - From Tectonics to Ice: Session in Honor of Austin Post, Paper 27-6. *In* "North to Alaska: Geoscience, Technology, and Natural Resources. 102nd Annual Meeting of the Cordilleran Section, GSA, 81st Annual Meeting of the Pacific Section, AAPG, and the Western Regional Meeting of the Alaska Section, SPE (8-10 May 2006),." Anchorage, Alaska.

Shennan, I., and Hamilton, S. L. (2006c). Late Holocene great earthquakes and relative land- and sea-level change: establishing regional correlations between Cook Inlet and the Pacific coast of south central Alaska. In: Bering Glacier to Glacier Bay - From Tectonics to Ice: Session in Honor of Austin Post, Paper 27-7. *In* "North to Alaska: Geoscience, Technology, and Natural Resources. 102nd Annual Meeting of the Cordilleran Section, GSA, 81st Annual Meeting of the Pacific Section, AAPG, and the Western Regional Meeting of the Alaska Section, SPE (8-10 May 2006),." Anchorage, Alaska.

Shennan, I., Hamilton, S. L., and Long, A. J. (2004). Late Holocene paleoseismicity and associated land/sea level change in the greater Anchorage area, pp. 55. Final Report to the U. S. Geological Survey.

Uchida, N., Hasegawa, A., Matsuzawa, T., and Igarashi, T. (2004). Pre- and post-seismic slow slip on the plate boundary off Sanriku, NE Japan associated with three interplate earthquakes as estimated from small repeating earthquake data. *Tectonophysics* **385,** 1-15.

Zong, Y., Shennan, I., Combellick, R. A., Hamilton, S. L., and Rutherford, M. M. (2003). Microfossil evidence for land movements associated with the AD 1964 Alaska earthquake. *The Holocene* **13,** 7-20.

7. Figures

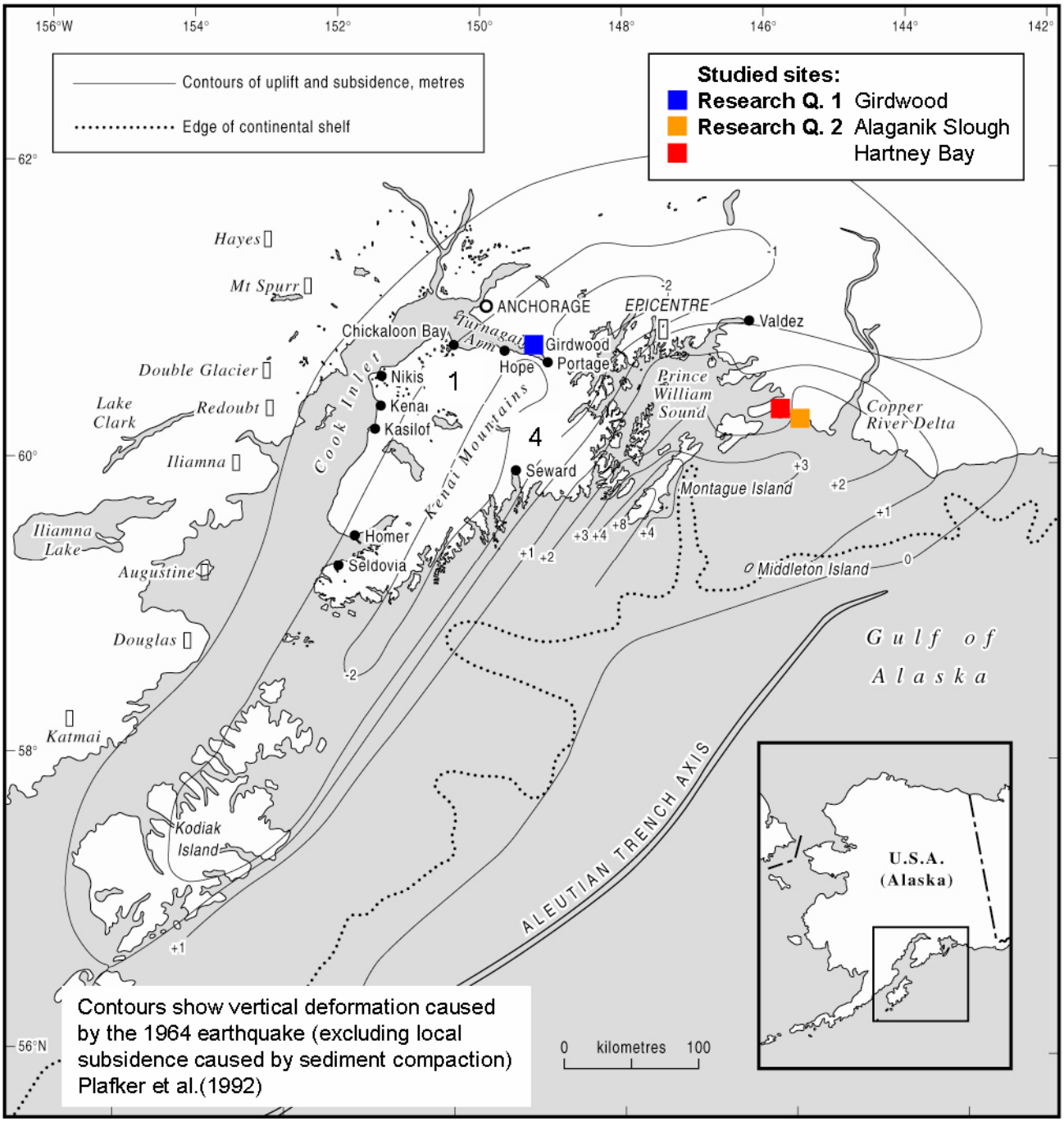

Figure 1 - Location of field sites, Girdwood and Copper River Delta. Contours show vertical deformation caused by the 1964 earthquake (excluding local subsidence caused by sediment compaction), modified from Plafker (1969).

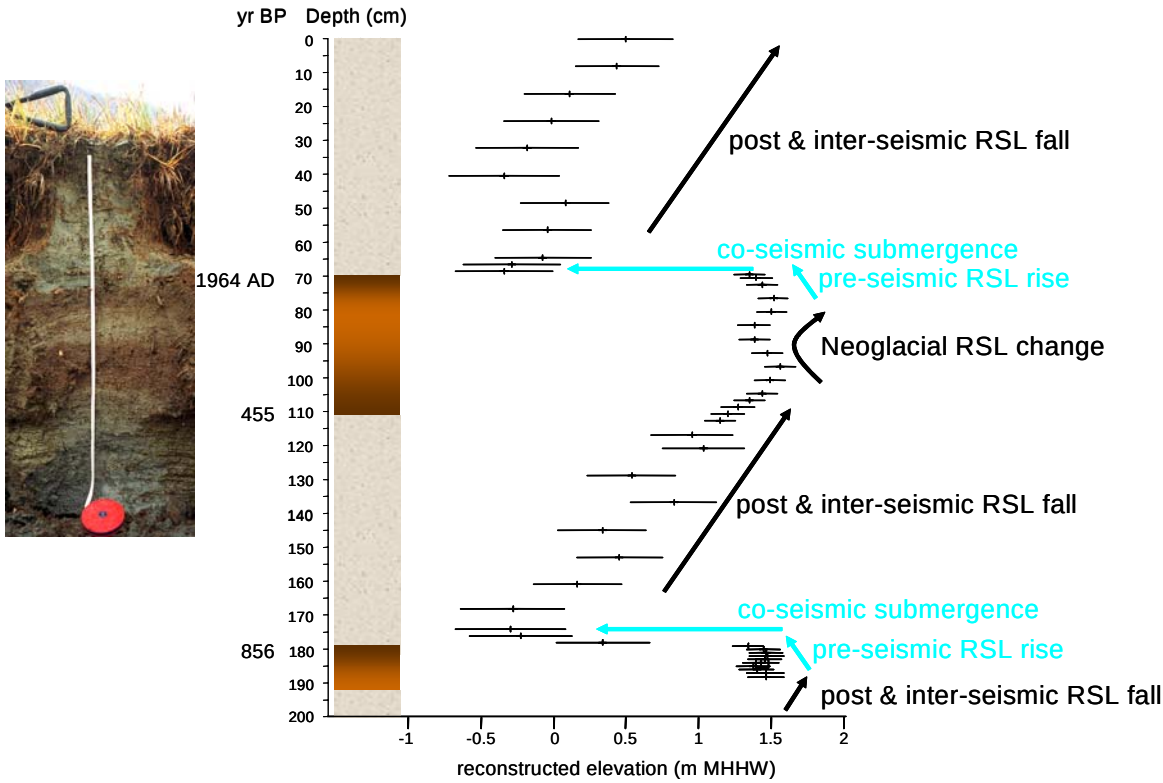

Figure 2 – Reconstruction of RSL change for Girdwood (core GW-1) showing the four phases of the earthquake deformation cycle.

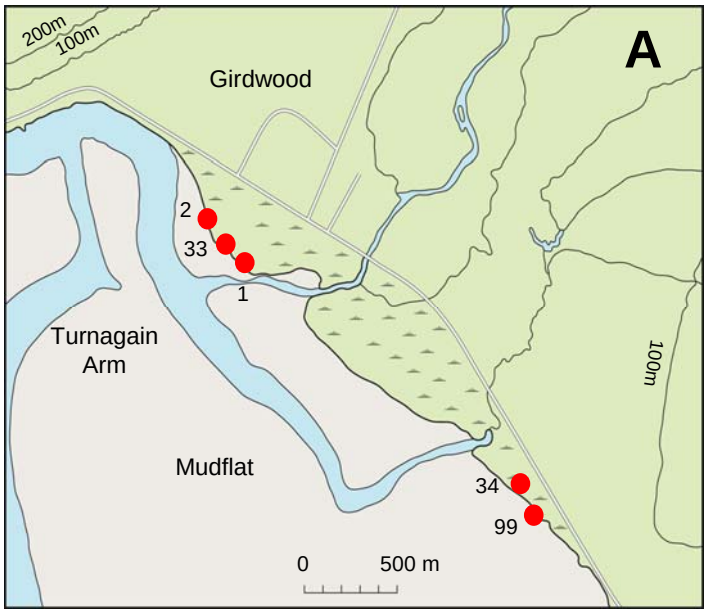

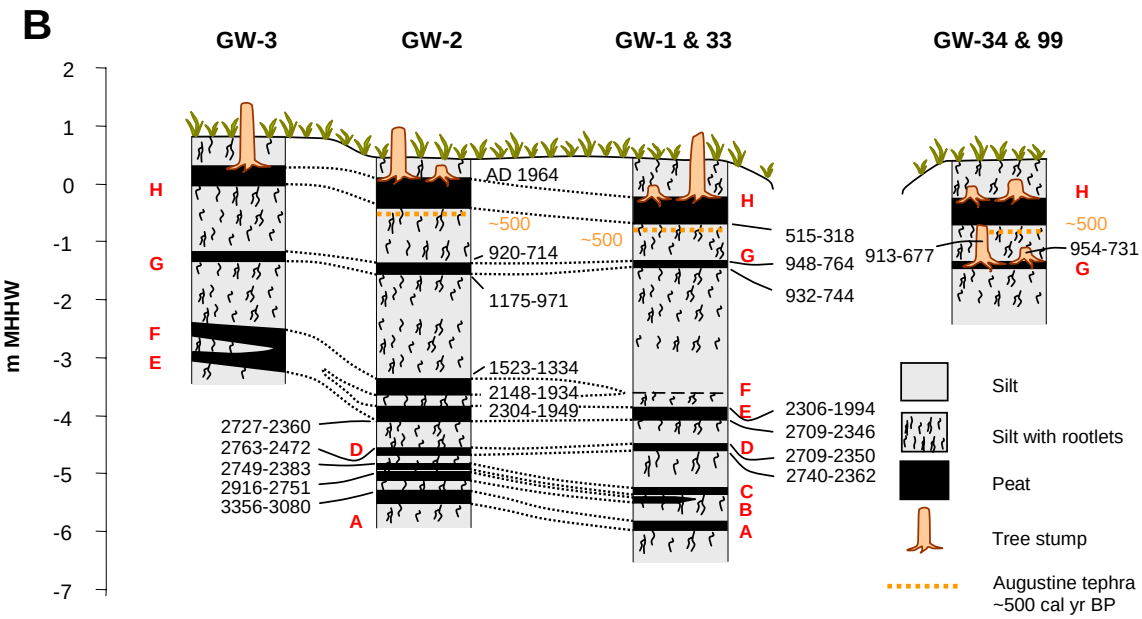

Figure 3 - (A) Detail of Girdwood sampling site showing locations of previous cores and sections. For general location of Girdwood, Turnagain Arm and Cook Inlet see Figure 1. Contours, at 100 m intervals, illustrate the alignment of the valley of Glacier Creek as it enters Turnagain Arm.

(B) Summary stratigraphy and ages of previously sampled sediments at Girdwood (Hamilton & Shennan, 2005a). Peat layers coded A to H and ages given as 95% probability range, years before present.

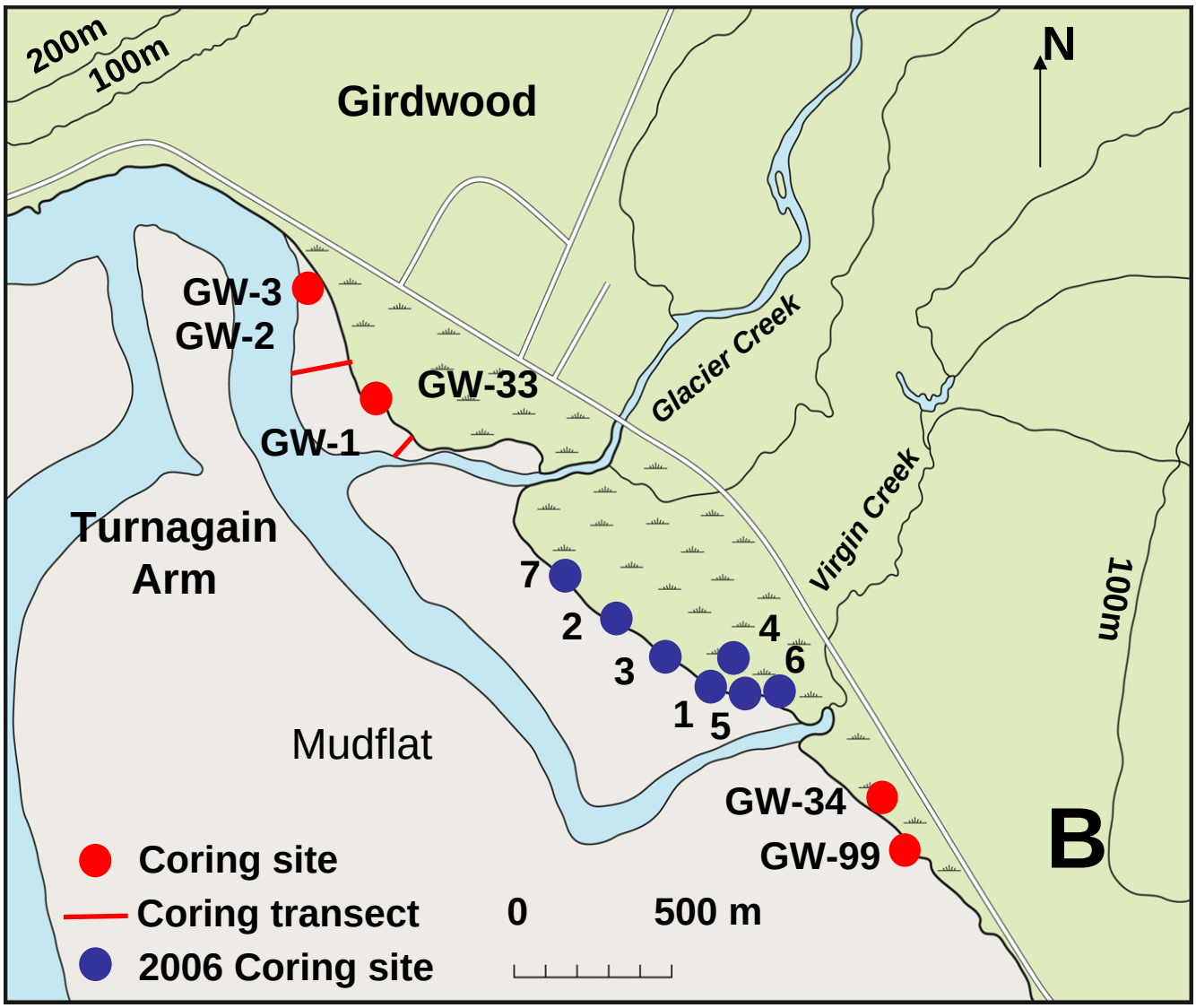

Figure 4 – Map of the location of the 2006 coring sites, plus previous core locations (Hamilton and Shennan, 2005a) at Girdwood marsh.

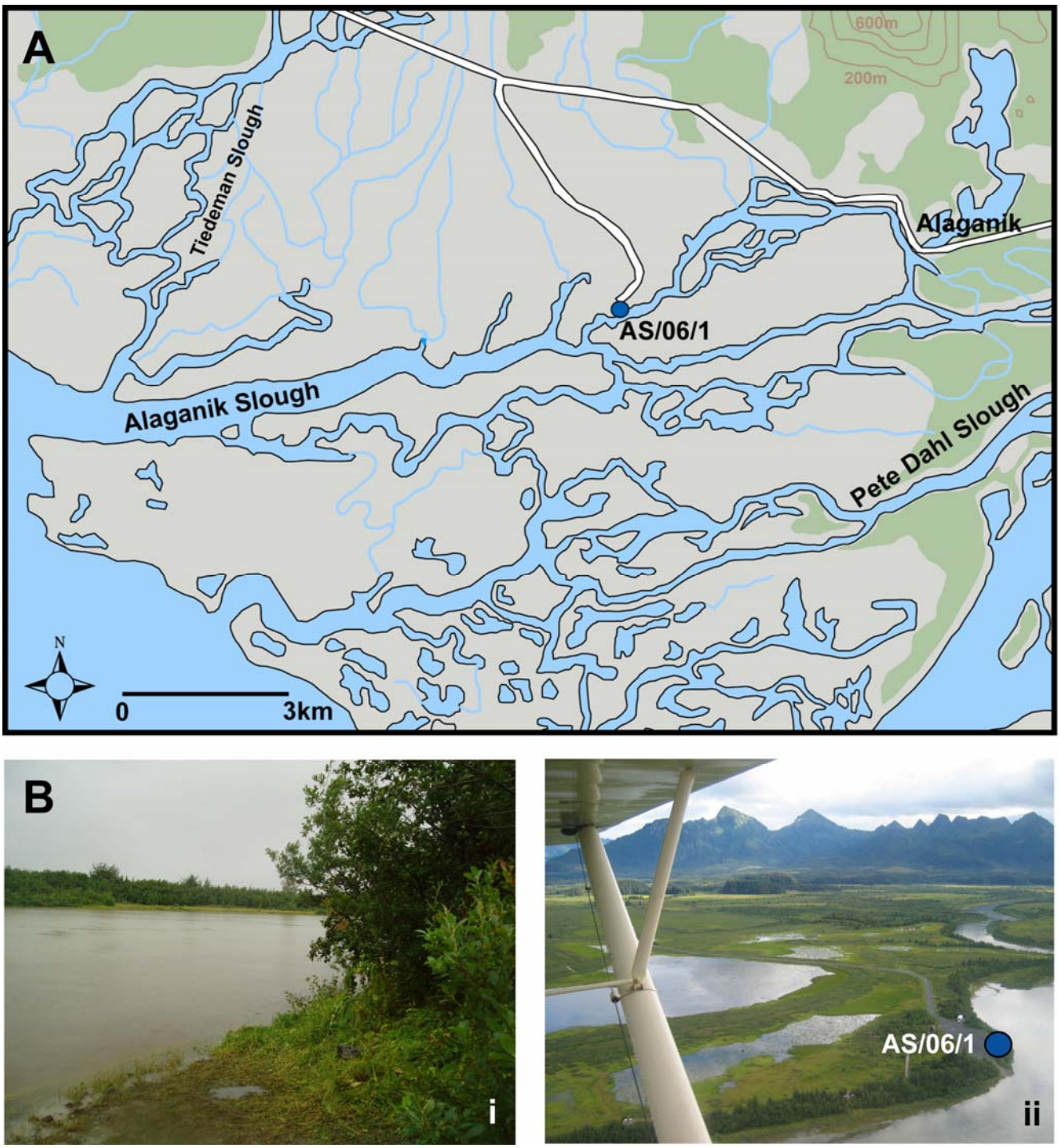

Figure 5 – (A) Location map of coring site AS/06/1 at Alaganik Slough, Copper River Delta.

(B) Photographs of AS/06/1 site; i – bank full Alaganik Slough at coring site; ii – aerial view of the bank full Alaganik Slough and site AS/06/1 from the small aircraft we chartered.

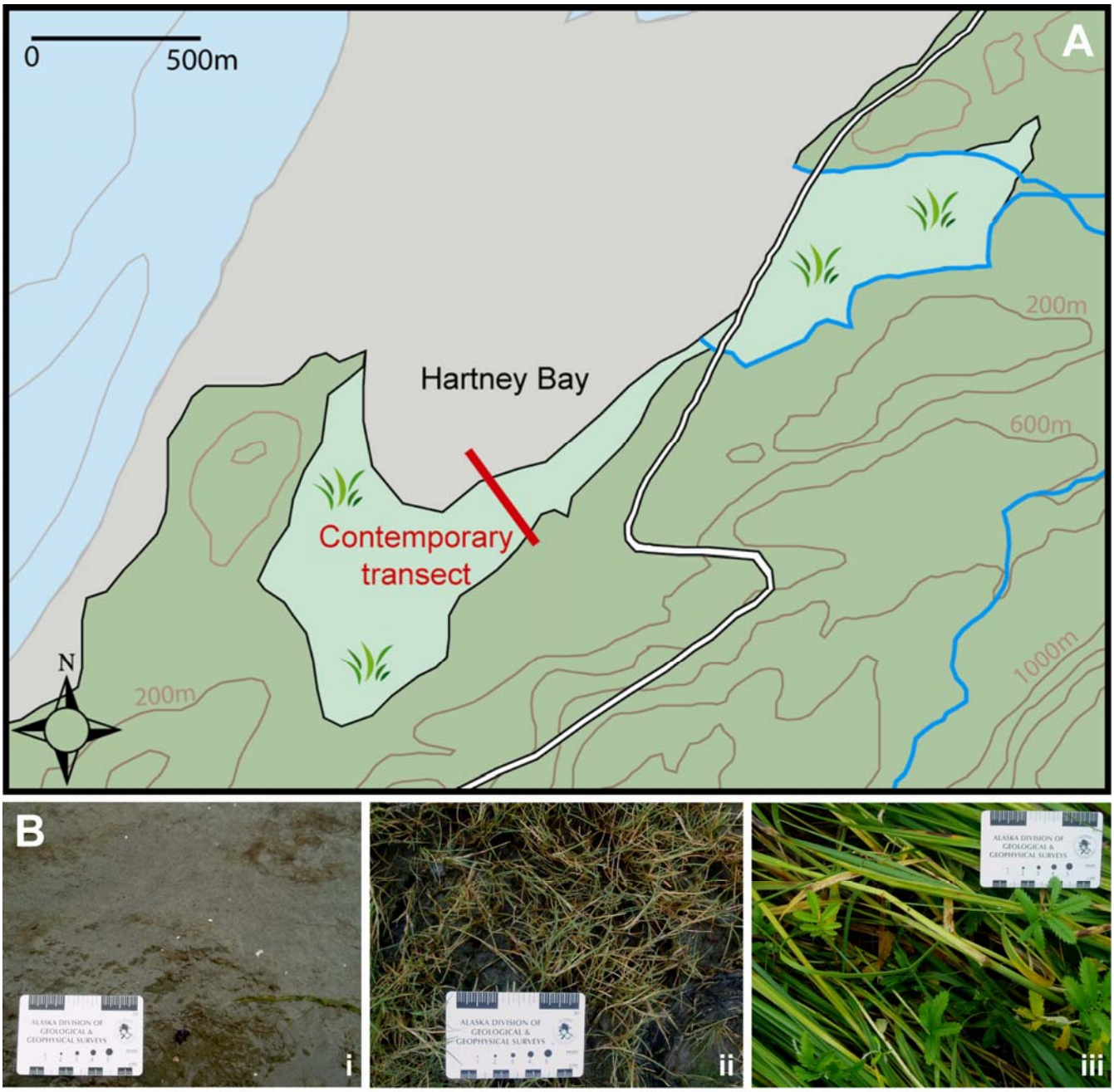

Figure 6 – (A) Location map of the transect of contemporary sediments collected at Hartney Bay, Cordova.

(B) Photographs of the contemporary sedimentary environments found along transect from which the twenty-two samples were collected: i – mud flat; ii – low marsh; iii – high marsh.

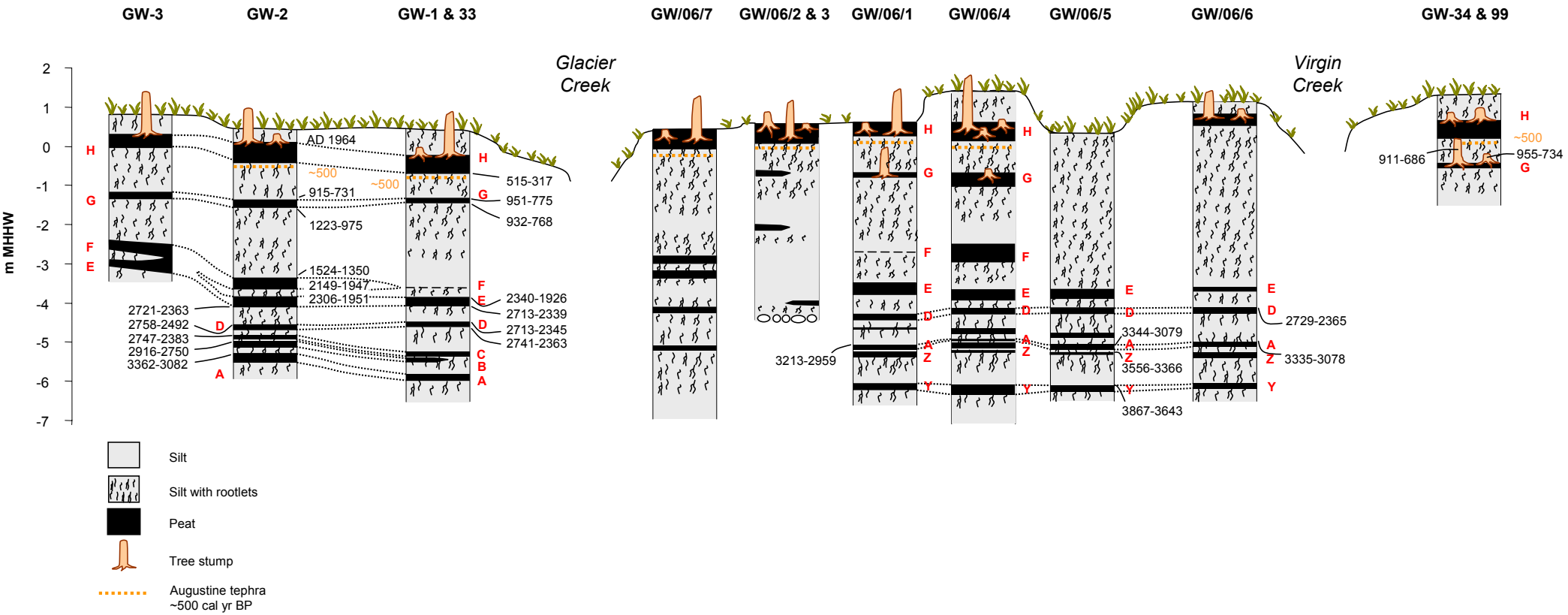

Figure 7 – Cross section of cores sampled at Girdwood showing buried peat layers below the surface. Peat layers coded Y to H and ages given as 95% probability range (Reimer et al., 2004) (Ramsey, 2001). Correlation of peat layers in the central section of the marsh (collected in 2006, prefix GW/06/, new radiocarbon results given in Table 2) and those on the north side of Glacier Creek (reported by Hamilton and Shennan, 2005) based on the shown radiocarbon ages and recorded diatom assemblages.

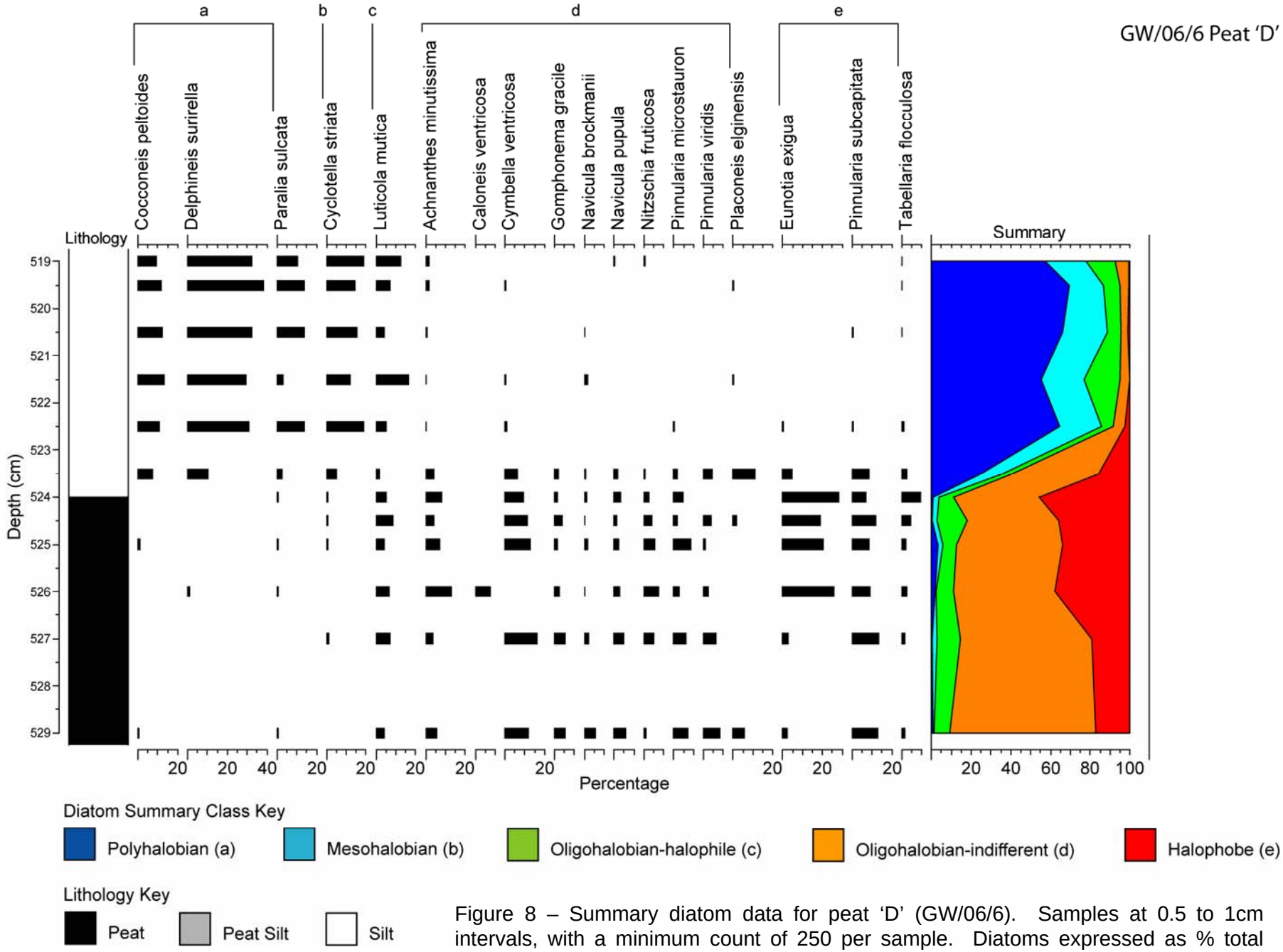

Figure 8 – Summary diatom data for peat 'D' (GW/06/6). Samples at 0.5 to 1cm intervals, with a minimum count of 250 per sample. Diatoms expressed as % total count, showing those species >5%.

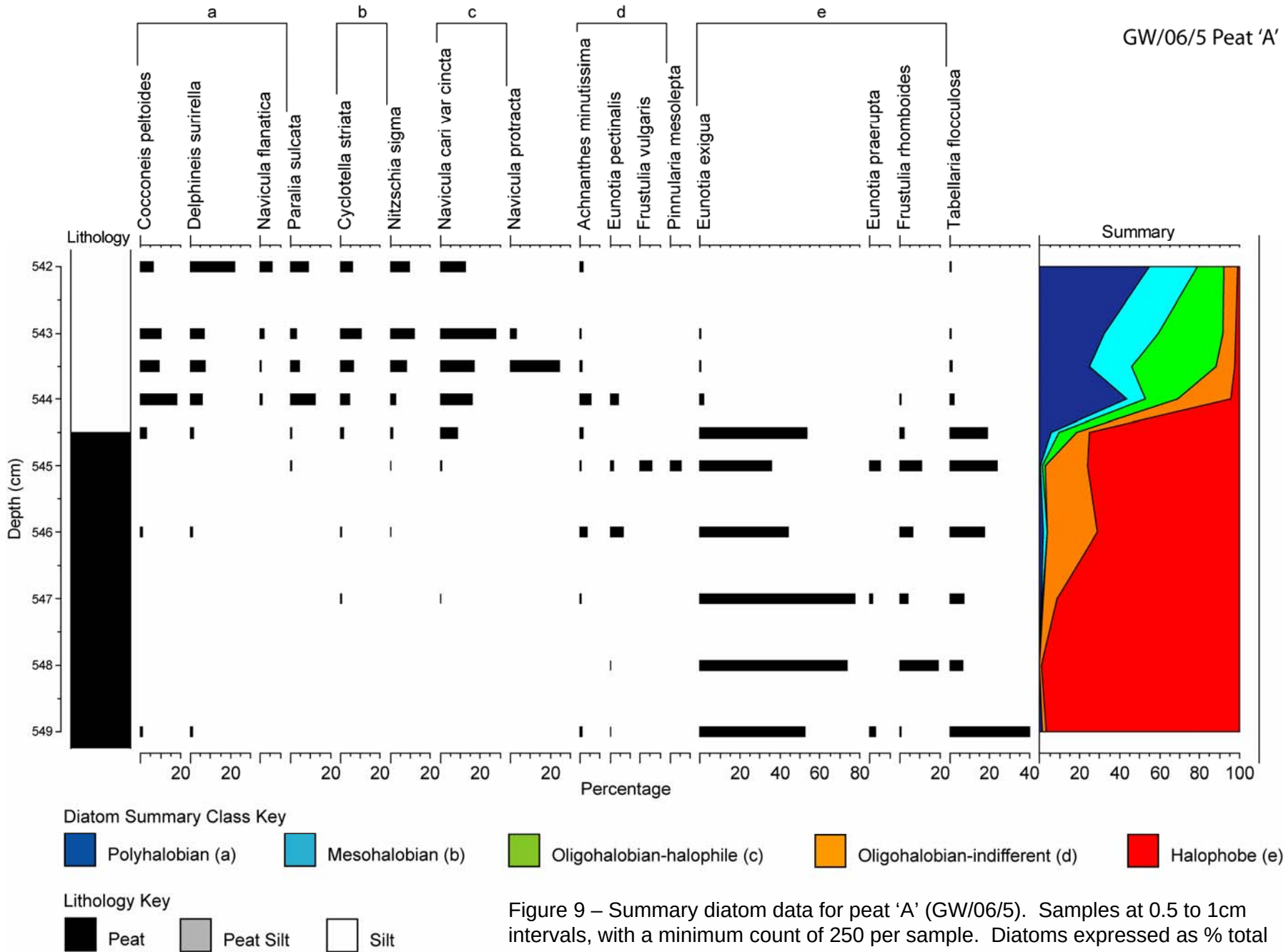

Figure 9 – Summary diatom data for peat 'A' (GW/06/5). Samples at 0.5 to 1cm intervals, with a minimum count of 250 per sample. Diatoms expressed as % total count, showing those species >5%.

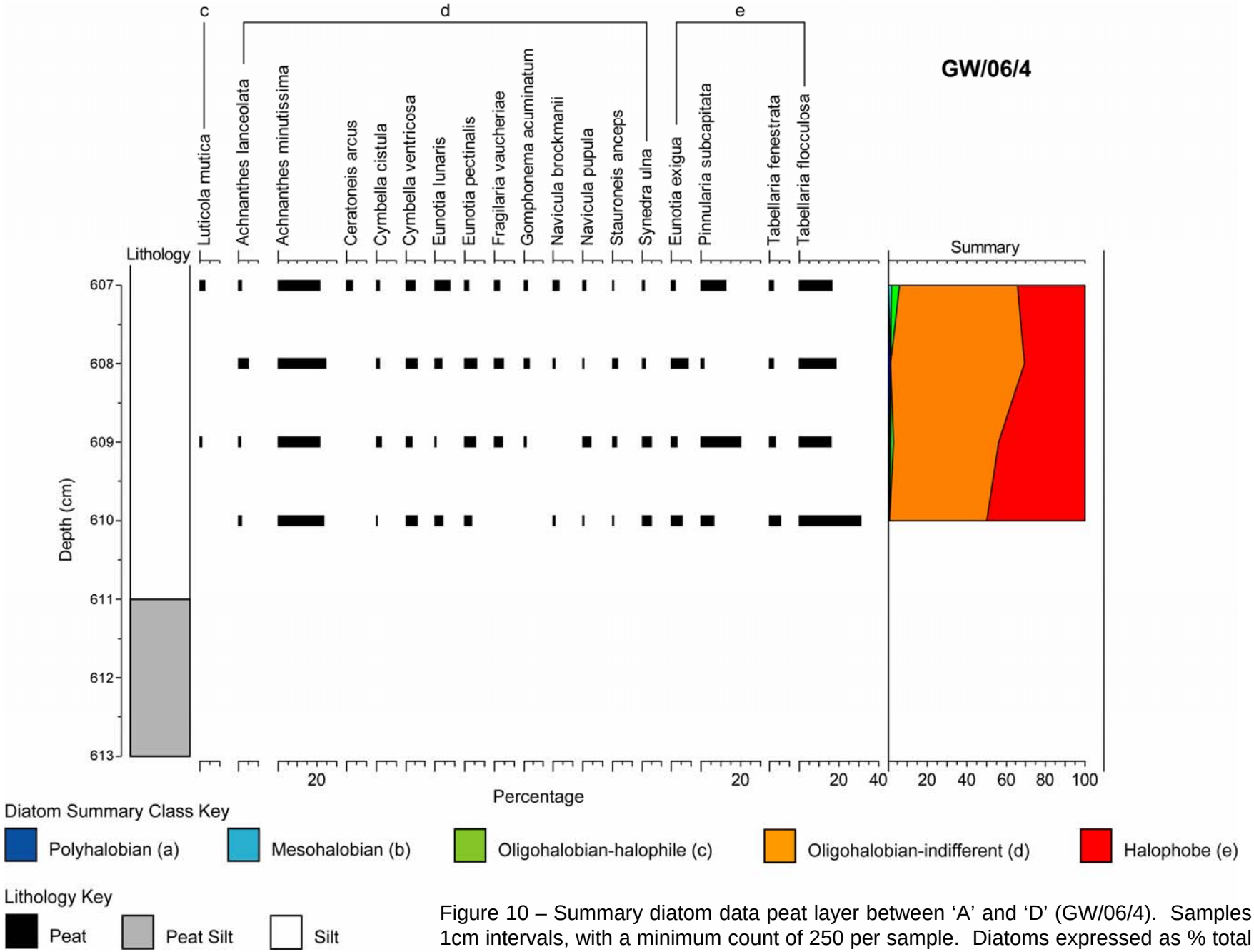

Figure 10 – Summary diatom data peat layer between 'A' and 'D' (GW/06/4). Samples 1cm intervals, with a minimum count of 250 per sample. Diatoms expressed as % total count, showing those species >5%.

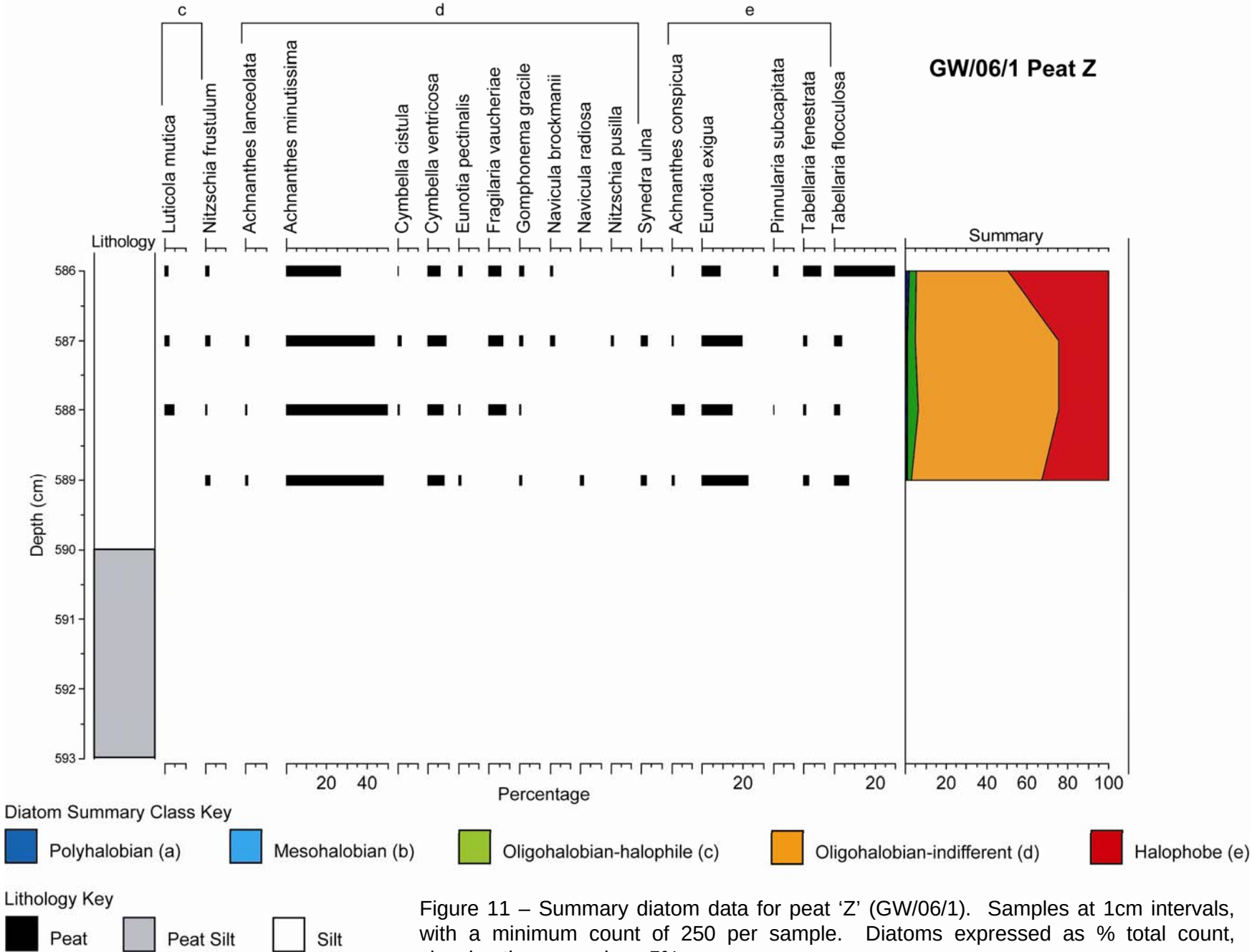

Figure 11 – Summary diatom data for peat 'Z' (GW/06/1). Samples at 1cm intervals, with a minimum count of 250 per sample. Diatoms expressed as % total count, showing those species >5%.

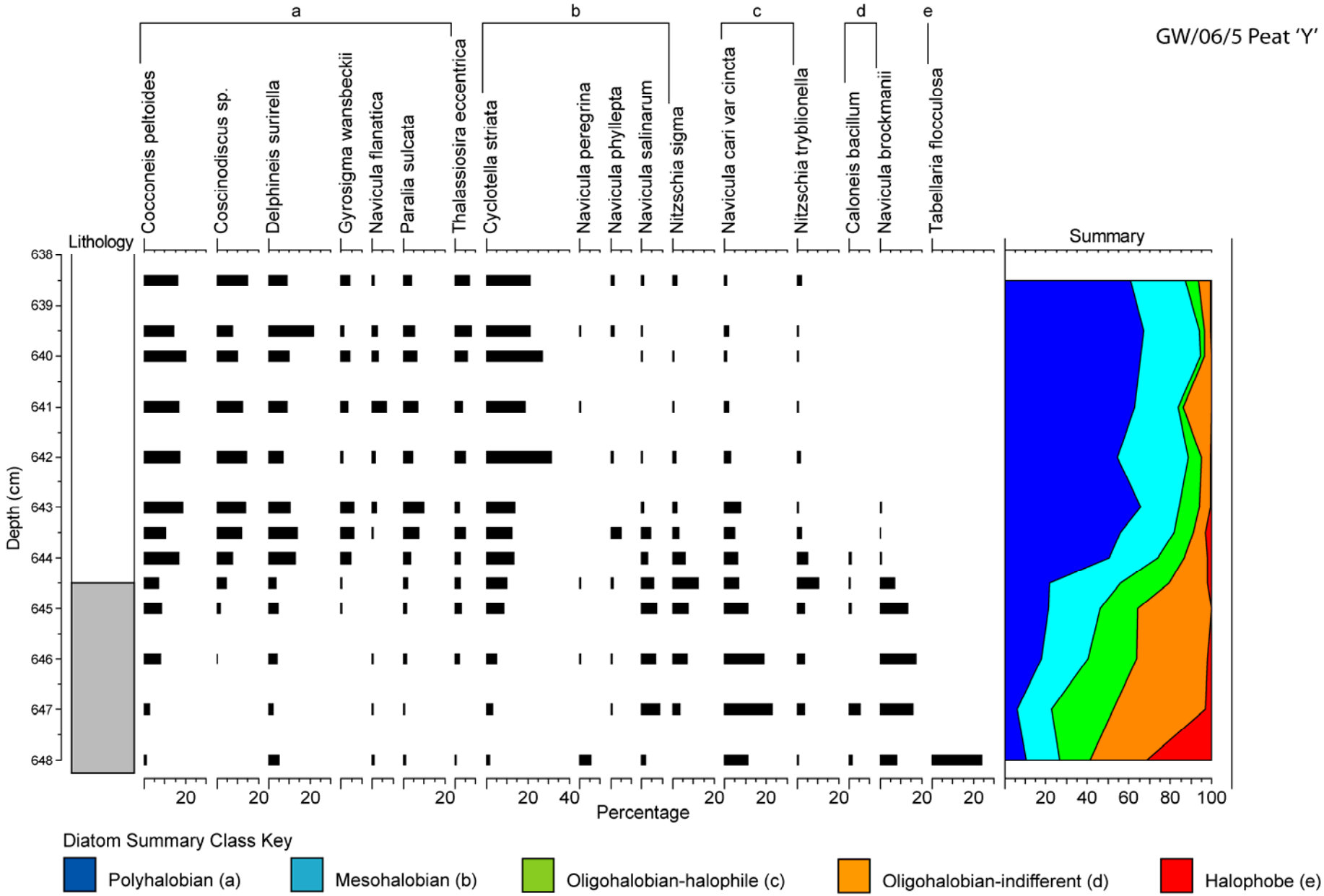

Figure 12 – Summary diatom data for peat 'Y' (GW/06/5). Samples at 0.5 to 1cm intervals, with a minimum count of 250 per sample. Diatoms expressed as % total count, showing those species >5%.

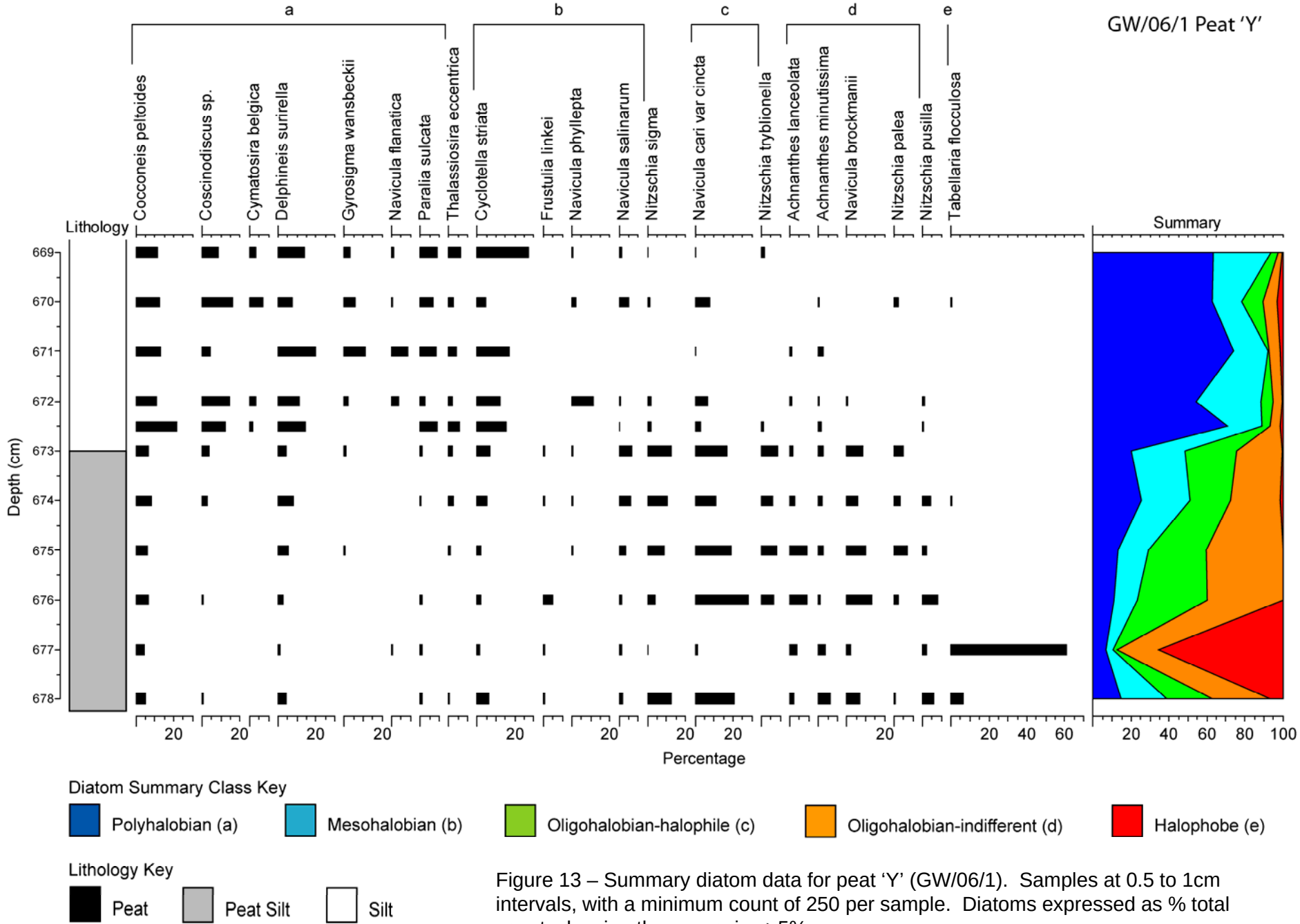

Figure 13 – Summary diatom data for peat 'Y' (GW/06/1). Samples at 0.5 to 1cm intervals, with a minimum count of 250 per sample. Diatoms expressed as % total count, showing those species >5%.

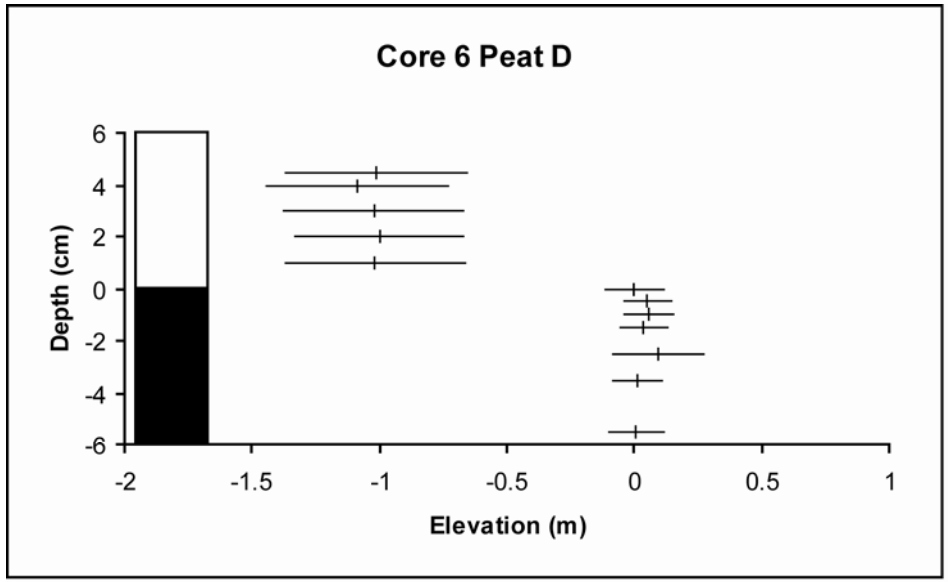

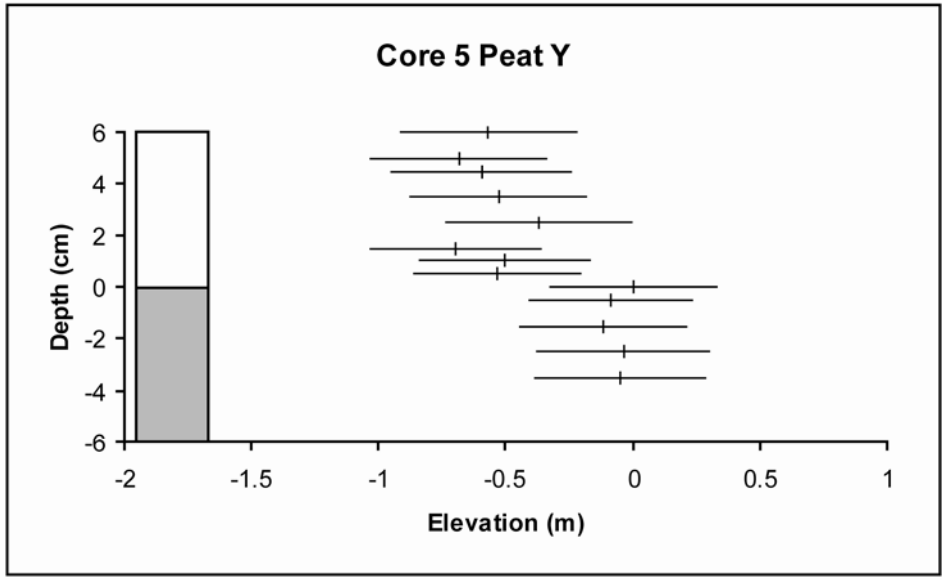

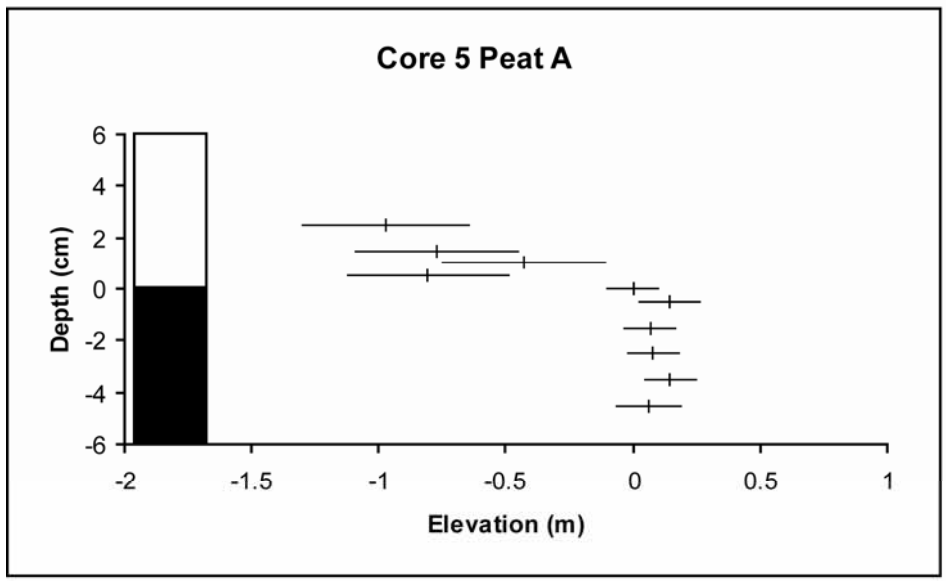

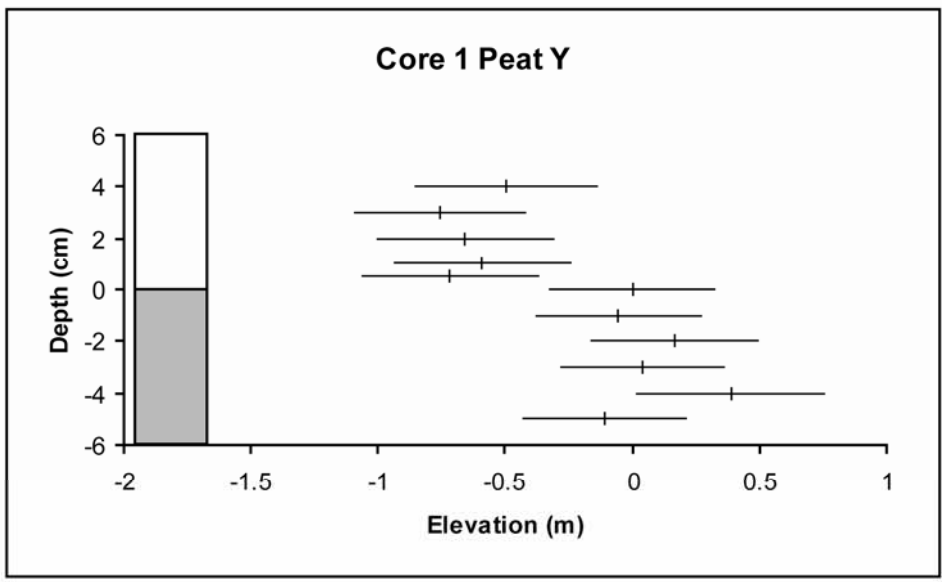

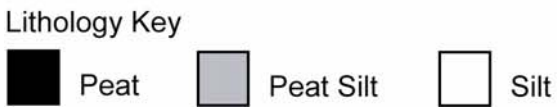

Figure 14 – Reconstructions of relative elevation ±1 standard error at Girdwood for peats D, Y and A. Graph for each earthquake standardised to change relative to the sample taken from the peat top.

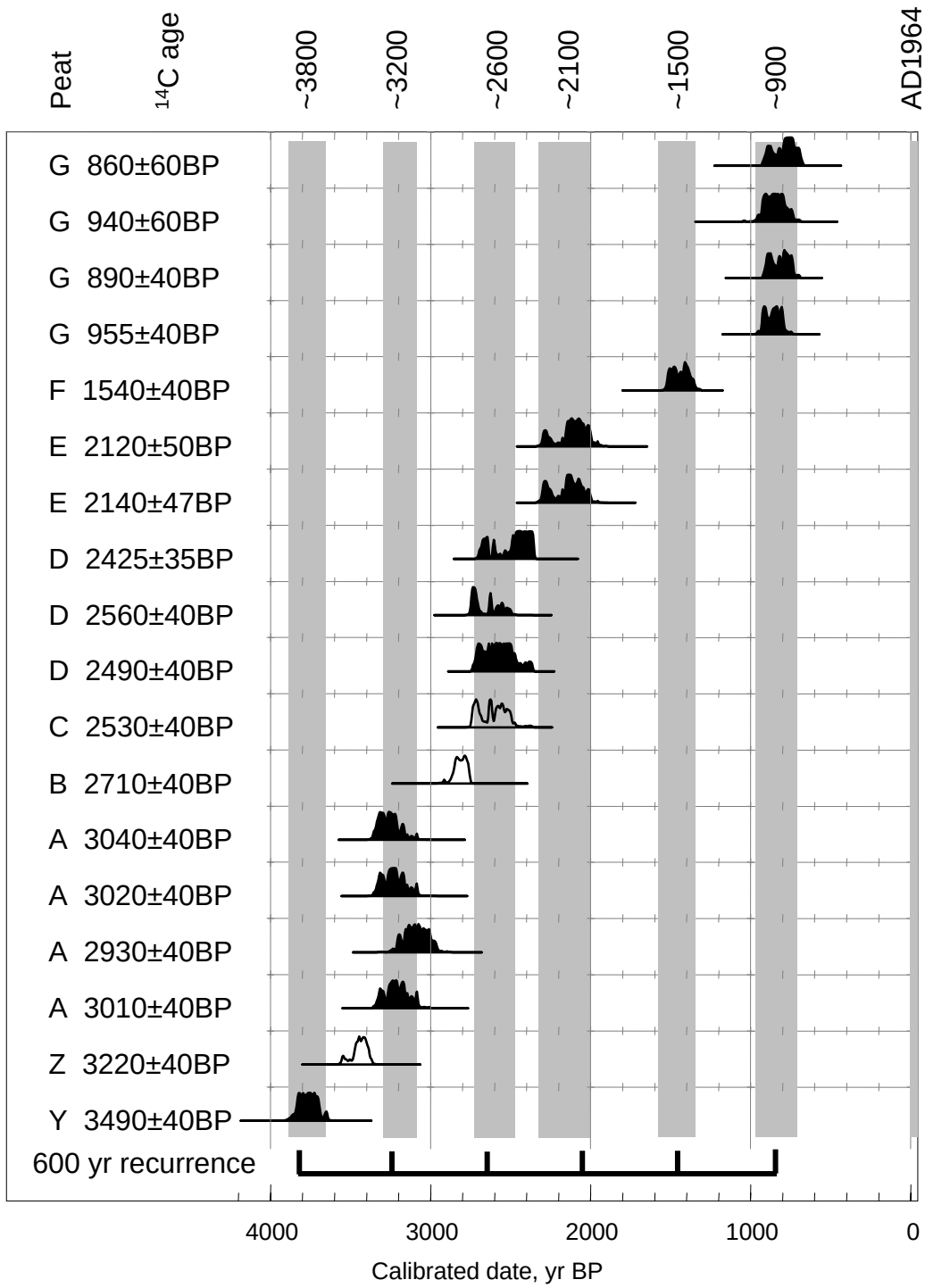

Figure 15 – Calibration of radiocarbon samples taken from the top of the peat layers submerged following co-seismic subsidence. Diatom analysis shows peat Z, peat B and Peat C (open histograms) do not record co-seismic submergence. All dates from in situ plant macrofossils or tree stumps rooted in a peat layer. Calibrations based on OxCal v3.10 (Reimer et al., 2004) (Ramsey, 2001). Shaded areas indicate 95% probability age range of great earthquakes ~900, ~1500, ~2100, ~2500, ~3200 and ~3800 cal yr BP.

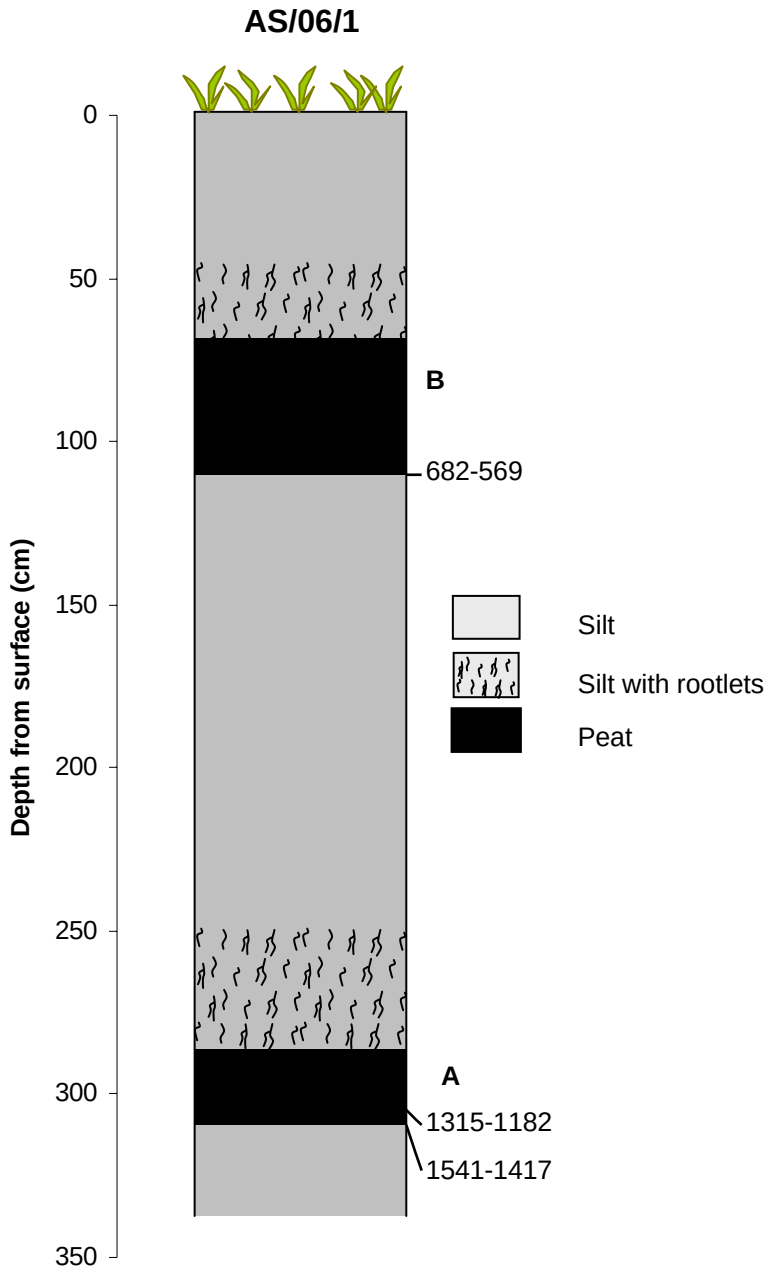

Figure 16 – Cross section of core sampled at Alaganik Slough showing buried peat layers below the surface. Peat layers labelled A and B and ages given as the 95% probability range (Reimer et al., 2004) (Ramsey, 2001).

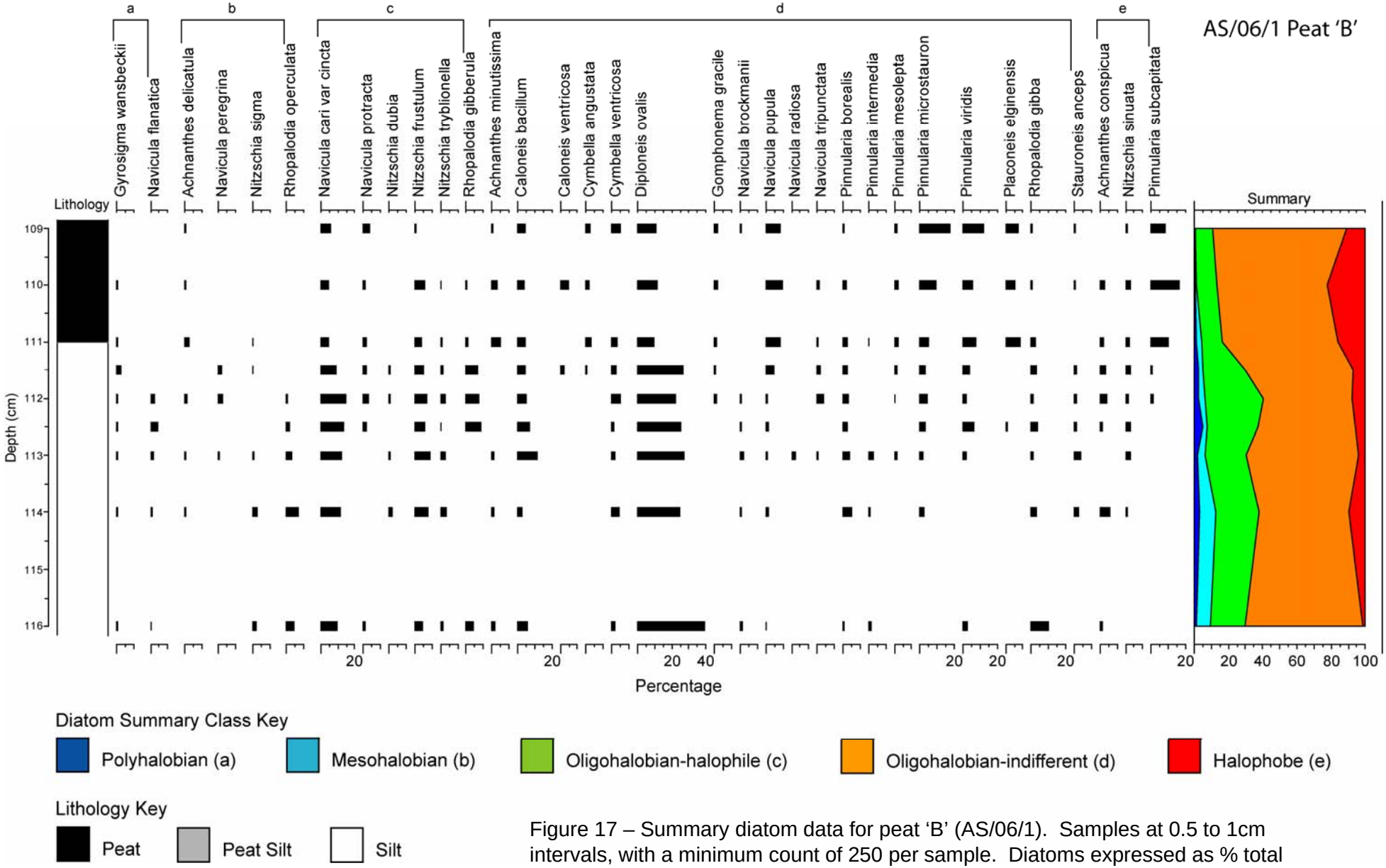

Figure 17 – Summary diatom data for peat 'B' (AS/06/1). Samples at 0.5 to 1cm intervals, with a minimum count of 250 per sample. Diatoms expressed as % total count, showing those species >2%.

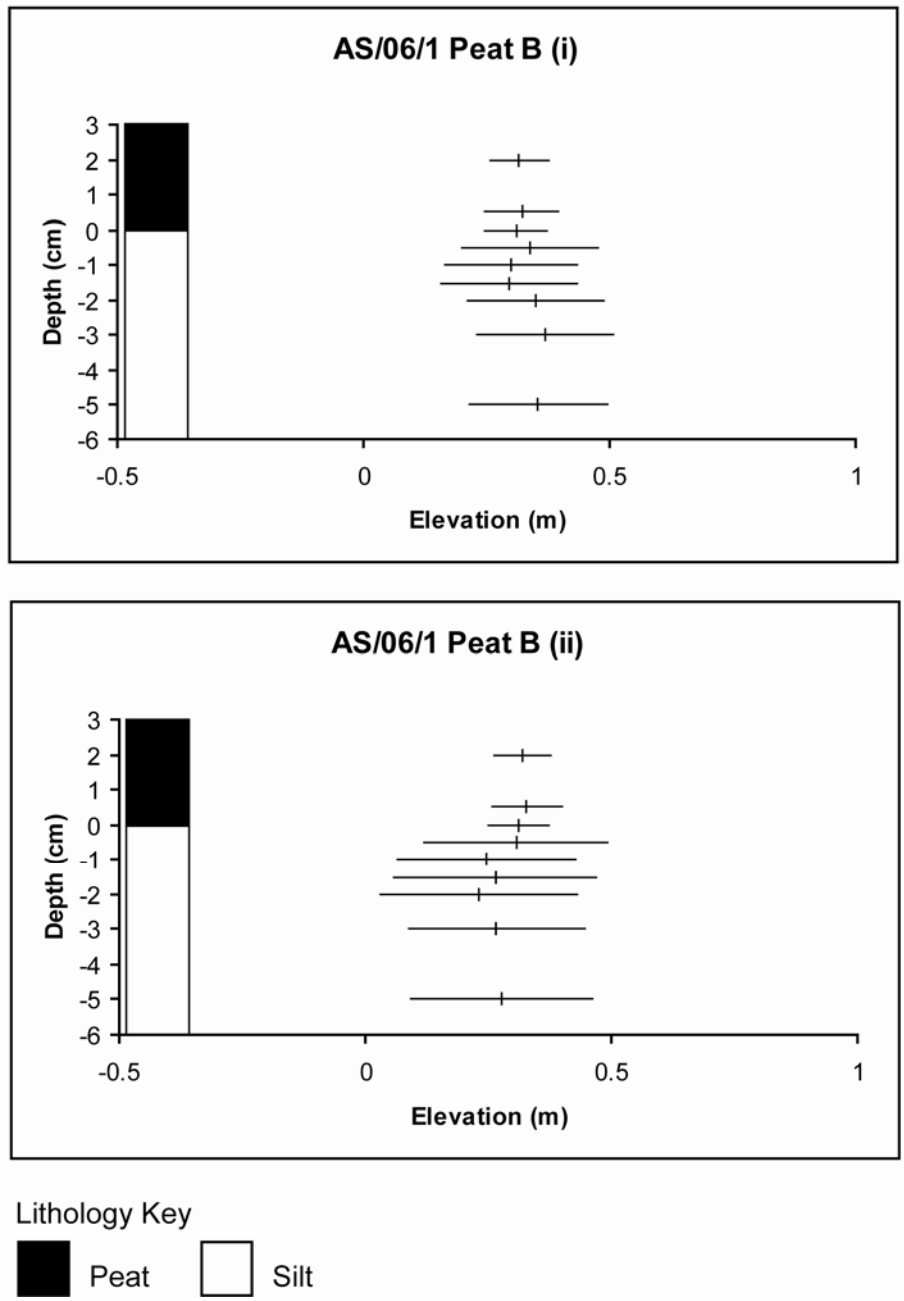

Figure 18 – Reconstructions of relative elevation ±1 standard error at Alaganik Slough for peat B. Graph for each earthquake standardised to change relative to the sample taken from the peat top. i – Reconstruction results from transfer function using upper Cook Inlet modern training set (Hamilton and Shennan, 2005). ii - Reconstruction results from transfer function using combined upper Cook Inlet modern training set (Hamilton and Shennan, 2005) and Hartney Bay contemporary samples.

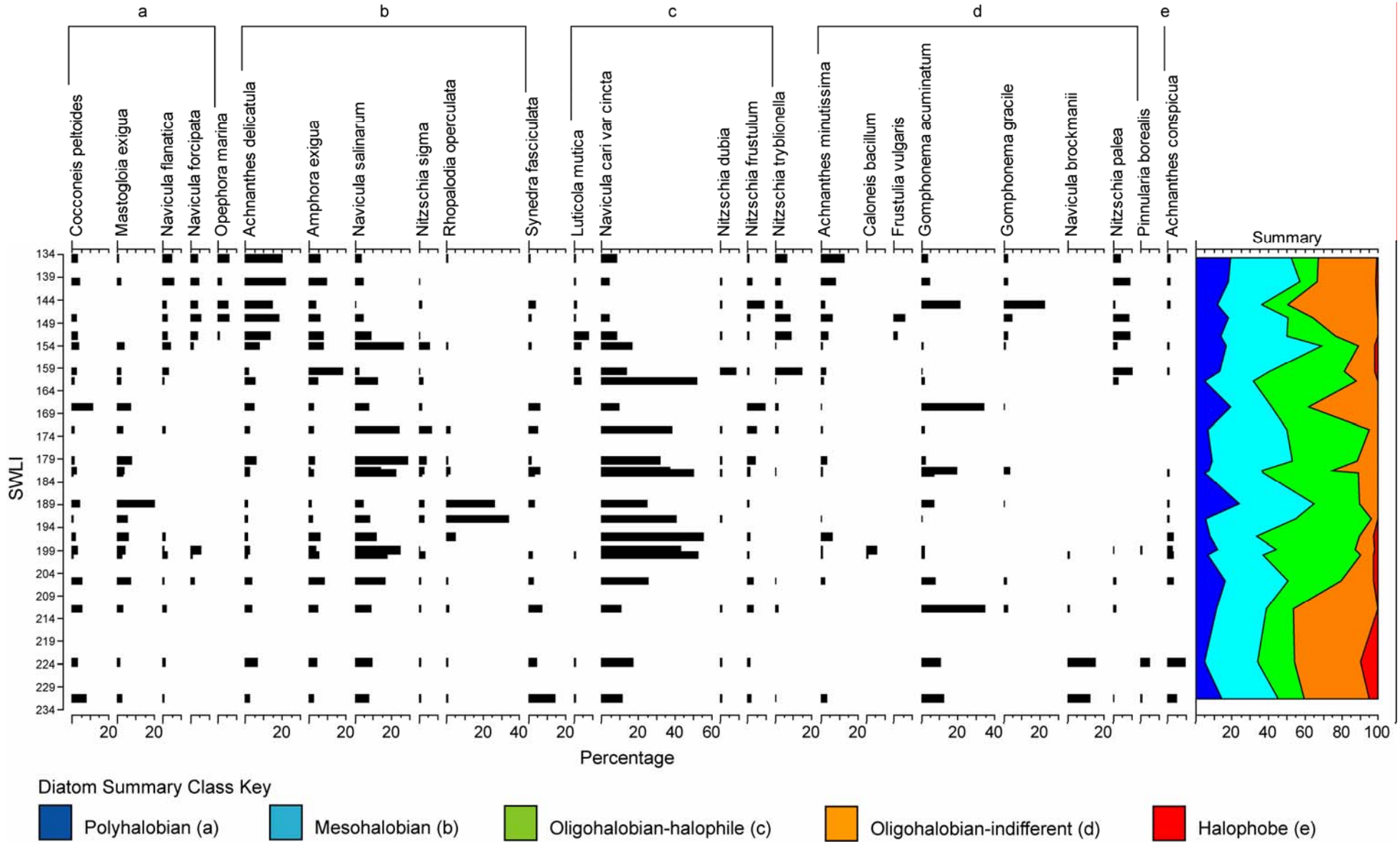

Figure 19 – Summary diatom data for modern samples from Hartney Bay against SWLI value. Samples with minimum count of 250 per sample. Diatoms expressed as % total count, showing those species >5%.

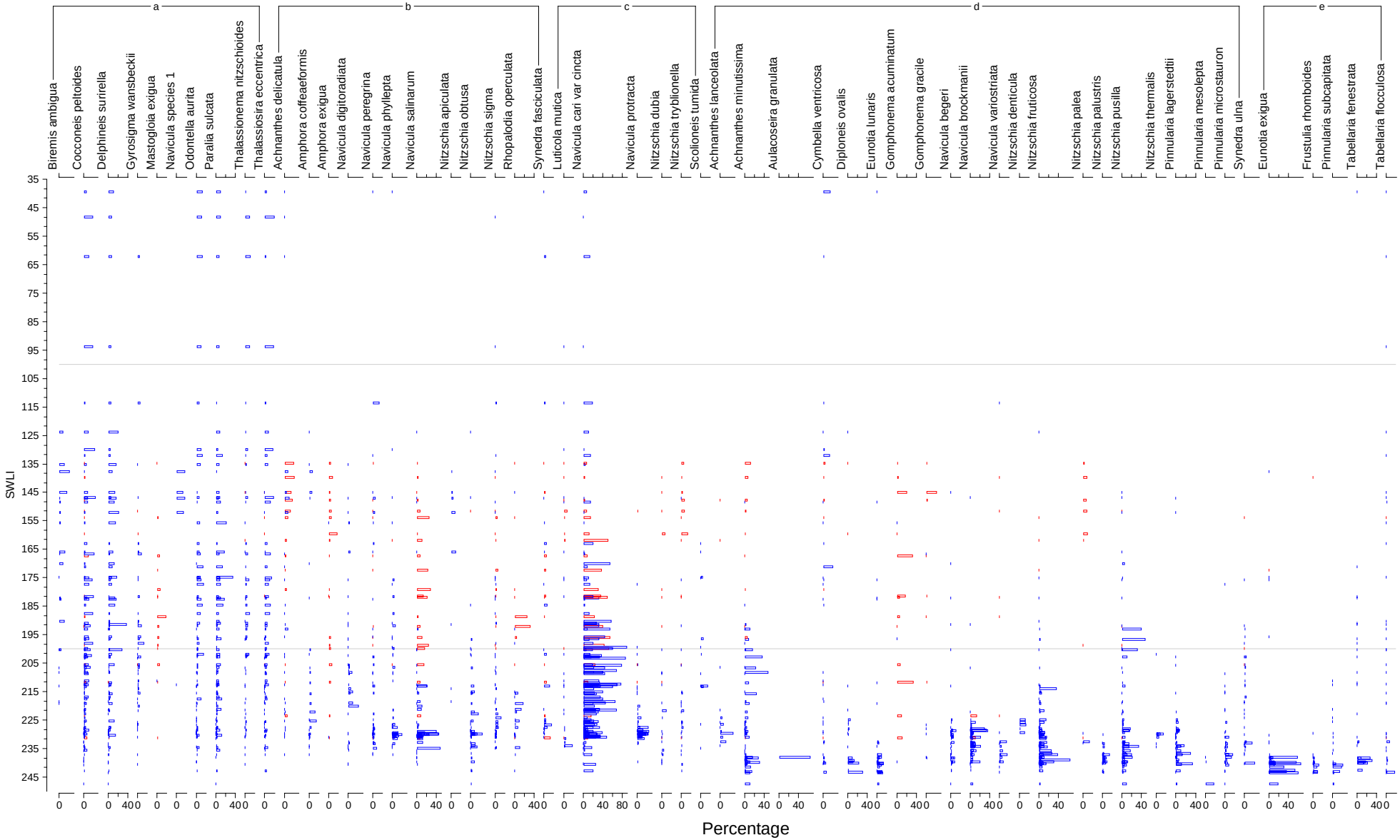

Figure 20 – Modern diatom data (≥15% total diatom valves counted) for **upper Cook Inlet** and **Hartney Bay**. Samples ordered by elevation (Standardised Water Level Index, where 100 = mean sea level and 200 = mean higher high water). Summary diatom classification: a – Polyhalobian; b – Mesohalobian; c – Oligohalobian-halophile; d – Olgiohalobian-indifferent; e – Halophobe

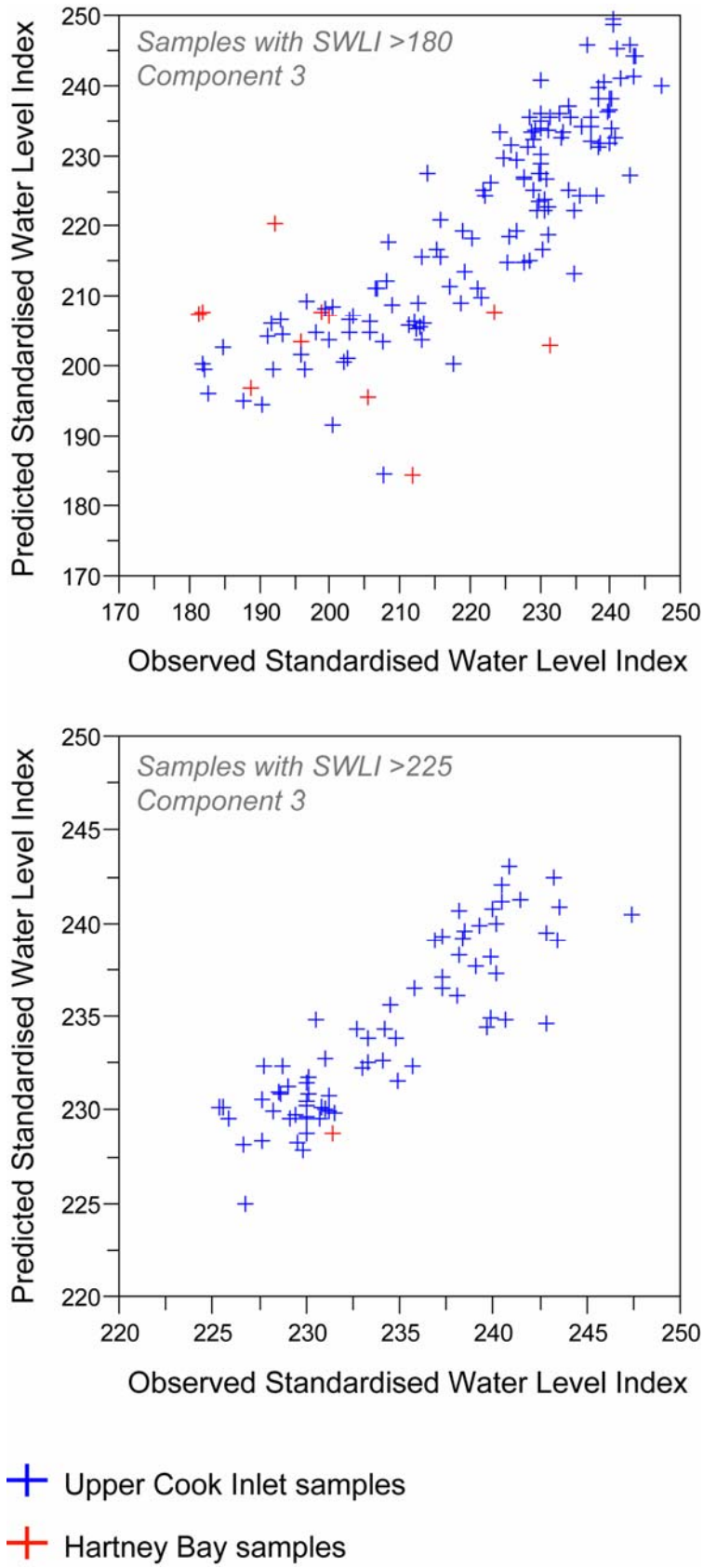

Figure 21- Observed against predicted Standardised Water Level Index (SWLI) values for the combined upper Cook Inlet (Hamilton and Shennan, 2005) and Hartney Bay modern training set for two transfer function models.

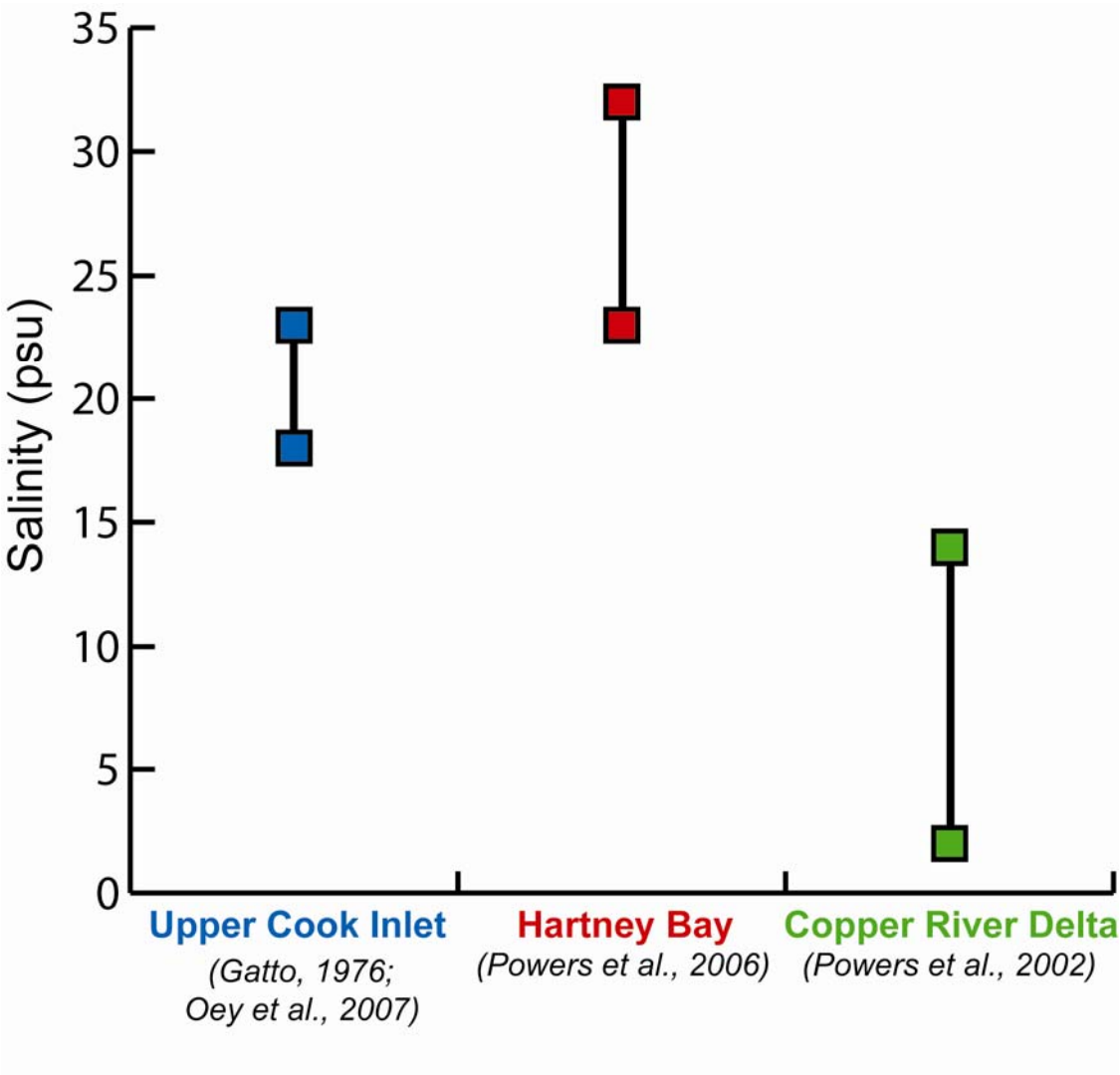

Figure 22 – Reported salinity ranges (as practical salinity units [psu]) for upper Cook Inlet, Hartney Bay and Copper River Delta.

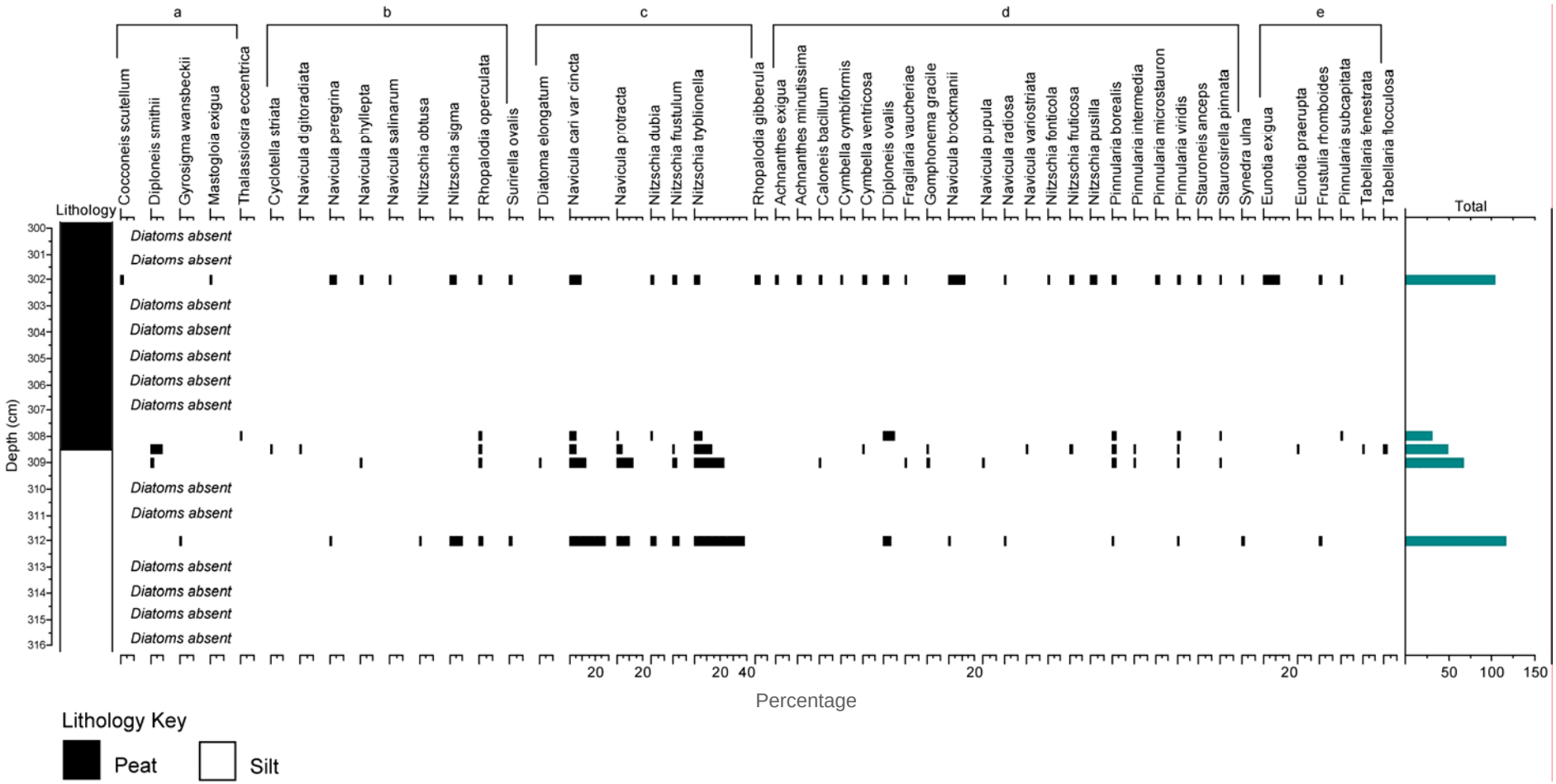

Figure 23 – Summary diatom data from peat A (AS/06/1). All data displayed as absolute values as no sample contained greater than 250 counts. Samples marked where no diatoms found to be present. Summary diatom classification: a – Polyhalobian; b – Mesohalobian; c – Oligohalobian-halophile; d – Olgiohalobian-indifferent; e – Halophobe